Chapter 4

Control

THE split of the continuous casting defect model into a manipulated variable (casting speed) to intermediate variable (temperatures) model (MVIV); and intermediate variable to output variable (defects) model (IVOV) was done to make control of defects possible. Feedback can now be applied using the MVIV model by measuring temperatures (now called "outputs") and applying control by manipulating casting speed (manipulated variable). Regulation of the temperatures at optimal set-points will ensure that defect formation is restricted (see §3.4.4), implying therefore that the defects can be controlled.

The control problem is therefore to control 38 thermocouple temperatures with 1 manipulated variable, casting speed, *i.e.* a SIMO (single-input/multiple-output) problem. If the effect of the manipulated variable on each of the outputs is not the same, the system is not completely output controllable *i.e.* every output can not be driven to a desired output in a finite time [167]. Since the effect of the manipulated variable is not the same on all thermocouples it is impossible, for this system, to achieve perfect control. This is highlighted by the fact that the rank of the output controllability matrix, $[\mathbf{CB} \quad \mathbf{CAB} \quad \mathbf{CA}^2\mathbf{B} \quad \ldots \quad \mathbf{CA}^{38}\mathbf{B}]$ [167], of the MVIV system defined in §3.3.1.5 is 7, 6, 6, and 5 for 1060, 1280, 1320 and 1575mm wide slabs respectively[a]. Since the ranks of the respective models are less than the dimension of the state vector (38), the system is not controllable [167]. The system is, however, stabilisable—because the uncontrollable subspace of the MVIV model is stable[b][169]. The MVIV system is fully state observable *i.e.* the rank of the observability matrix [167] is equal to the dimension of the state vector (38).

[a] These ranks were calculated using the MATLAB Control Systems Toolbox [168].

[b] the whole system is in fact stable.

Because of the controllability limitations of the system a control strategy must be used that makes a trade-off between the quality of control on each of the outputs (intermediate variables). Three such linear controllers will be used to investigate the viability of control of this particular system. Linear control is used because the system can be adequately modelled as a linear time-invariant (LTI) system as shown in chapter 3. The controllers are as follows:

- linear quadratic tracker at steady-state,
- single-output control and
- worst-case control.

The linear quadratic tracker attempts to track the reference inputs as closely as possible on a weighted average basis while maintaining system stability for a LTI system. This has been described by Lewis [170] and an example application for an inverted pendulum (SIMO system) is given in Lewis [148]. The design is usually carried out for steady-state conditions and then used as a sub-optimal tracker for the dynamic case.

The single-output control utilizes the fact that one input should definitely be able to control one output. Therefore, one loop is closed and all other loops are open. The closed-loop output will track the reference input very closely (because that sub-system is controllable), and is only limited by actuator constraints. The disadvantage of this configuration is that only one output is tracked and no true control is applied to the other loops. It is hoped that the overall performance of the system will improve if the right loop is chosen to be closed. No references to this control approach could be found.

The worst-case control utilizes a switching strategy. Controllers are designed for each loop as if each loop is a single-input, single-output (SISO) system. Once an output error is performing at the worst level compared to the error of the other outputs, the controller switches from the active loop to the loop with the worst error, and controls that output. Once the output has improved to a level such that another output has become worse than the current output, the controller switches to that loop and the cycle repeats. Similar strategies can be found in papers by Sun, Ge, and Lee [171], Zhao and Spong [172] and Kordona, Dhurjatia, Fuentesb, and Ogunnaikeb [173]. The strategy is used to prevent any output from straying too far from the reference input. Problems of bump-less transfer [174] and integral windup are prevalent in this control configuration and are addressed in what follows.

The three controllers described above and their performance through simulation will be discussed in this chapter.

4.1 Linear quadratic tracker at steady-state (LQTSS)

This section describes the use of a linear quadratic tracker at steady-state (LQTSS) as a controller for the MV to IV model described in §2.2.5.

4.1.1 Implementation issues

The implementation of such a controller on a real plant is depicted in Fig. 4.1. In this

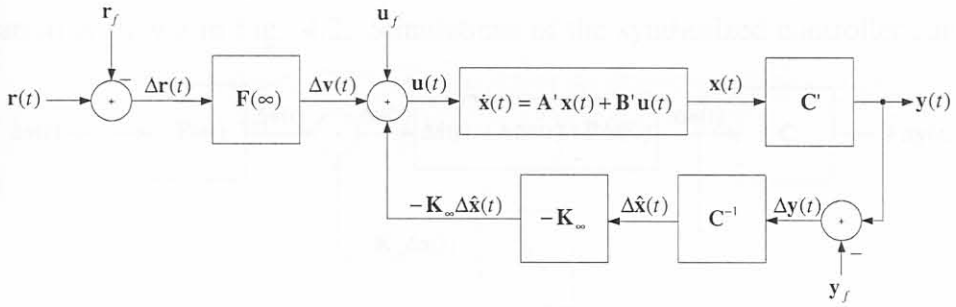

Figure 4.1 Implementation of the LQTSS in practice.

realization, the system $(\mathbf{A}', \mathbf{B}', \mathbf{C}')$ is the actual plant; and $\mathbf{u}(t)$, $\mathbf{x}(t)$ and $\mathbf{y}(t)$ are the true plant inputs, states and outputs respectively. Disturbances are left out at this stage for design purposes.

The "Δ" indicates deviational values of the respective variables and are needed, even in the practical realization since the identified model (and therefore the designed controller) is based on the deviations of parameters from set values.

As an example, if $\mathbf{r}(t)$ denotes the true desired temperature for the system, $\Delta\mathbf{r}(t)$ denotes the deviation of the desired temperature for the system and is calculated by subtracting the offset value from the true value ($\Delta\mathbf{r}(t) = \mathbf{r}(t) - \mathbf{r}_f$).

The deviational estimate of the state of the system ($\Delta\hat{\mathbf{x}}(t)$) is determined by multiplying the measured deviational output, $\Delta\mathbf{y}(t)$, with the inverse of the $\mathbf{C}$ matrix of the identified model since the system has been identified as first order with outputs and states equal.

$\mathbf{F}(\infty) = \mathcal{L}^{-1}\{\mathbf{F}(0)\}$ denotes the time invariant feed-forward gain of the controller and $\mathbf{K}_\infty$ denotes the feedback gain.

A typical sequence of events which might be carried out by a controller is informative to

understand the practical controller structure. The output is measured and the deviational value of the output is determined using the offset value for that output. This value is then multiplied by the C matrix of the *identified* model to give an estimate of the deviational state of the system. The deviational state is then used in the state-feedback realization and multiplied by the feedback gain. The result is added to the feed-forward component. The feed-forward component is determined by multiplying the deviational desired value for the output with the feed-forward gain. The deviational control is then added to the offset value to determine the true control and is then used as the input to the true system.

For simplicity, the control system can be described by the deviational parameters only. This configuration is shown in Fig. 4.2. Simulations of the synthesized controller can be done

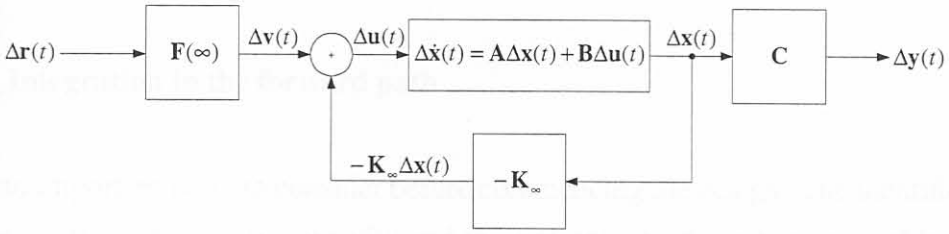

Figure 4.2 Analysis of the deviational LQTSS controller.

using the structure depicted, but care should be taken then when adding and subtracting offsets when the controller is implemented. The inverse of the C′ matrix has been dropped from the figure for the sake of simplicity.

4.1.2 Design overview

Using the design procedure depicted in Fig. 2.22 on page 51, one can now set about to design the LQTSS. Although there are four widths, 1320 and 1280mm wide slabs have very similar models and only the 1280mm wide slabs will be tested. Since there are now three versions of the MVIV models[c], three separate controllers have to be designed.

4.1.2.1 Specifications

The general specification is to design controllers to improve set-point tracking[d] (and thereby reduce the amount of defects) given the optimal set-points, measured disturbances, actua-

[c] 1060mm, 1280 to 1290mm and 1575mm widths

[d] in terms of the SMSMSE in §4.1.2.6.

tor constraints, and the MVIV model. Perfect set-point following is not possible, because the system is not completely output controllable. Mould level and water inlet temperature disturbance rejection should occur in the significant frequency band of the disturbances (see §4.1.4), while a maximum casting speed constraint of 1500mm/min and maximum absolute casting acceleration (slew rate) of 1000 mm/min^2 should not be exceeded.

Note that a controller which forces a decrease in casting speed causes lower throughput of cast product. The quality of cast product is however also important and a trade-off between quality and throughput has to be made. In this work it is assumed that quality is more important and decreases in casting speed are allowed. As will be seen in the remainder, reductions in casting speed are rare for all three types of controllers.

4.1.2.2 Integration in the forward path

There is an important point to consider before commencing the design. The identified model is predominantly first order (*i.e.* type 0); and this presents steady-state error problems in any feedback control scheme [149]. The system is SIMO, that is, it has one input and several outputs. Therefore, an ideal (zero) steady state solution for tracking the reference inputs by the outputs is impossible to achieve. However, the error in this case is the difference between the feed-forward and feedback signals: $\Delta\mathbf{u}(t) = \Delta\mathbf{v}(t) - \mathbf{K}_\infty\Delta\mathbf{x}(t)$; and the designer is in this case interested in having zero steady-state error for this difference. This implies that the *weighted* outputs will track the *weighted* set-points of each of the temperatures by manipulating the input (casting speed).

Since the system is first order, it is necessary to add an integrator in the forward path of the system to ensure that the weighted step reference ($\Delta v(t)$) is followed exactly (type 1). The compensating approach is depicted in Fig. 4.3. In the figure, the state of the original

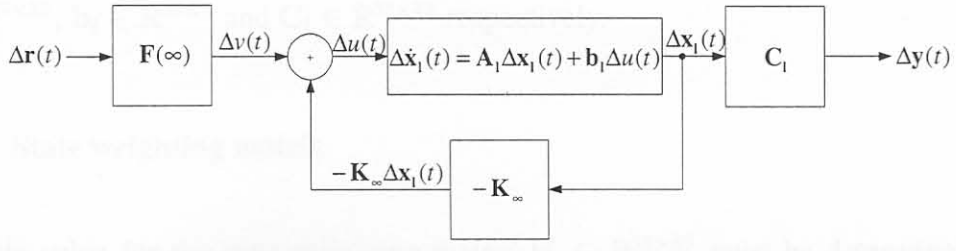

Figure 4.3 Addition of an integrator to the LQTSS.

system represented by the system $(\mathbf{A}, \mathbf{b}, \mathbf{C})$ has been augmented by an integrator of the form

$(a = 0, b = 1, c = 1)$. The compensator plus plant can be represented in state-space by the following system $(\mathbf{A}_1, \mathbf{b}_1, \mathbf{C}_1)$ as

$$\mathbf{A}_1 = \begin{bmatrix} 0 & \emptyset \\ \mathbf{b} & \mathbf{A} \end{bmatrix} \quad \mathbf{b}_1 = \begin{bmatrix} 1 \\ \emptyset \end{bmatrix} \quad \mathbf{C}_1 = \begin{bmatrix} \emptyset & \mathbf{C} \end{bmatrix}, \tag{4.1}$$

and

$$\Delta\dot{\mathbf{x}}_1(t) = \mathbf{A}_1\Delta\mathbf{x}_1(t) + \mathbf{b}_1\Delta u(t) \tag{4.2}$$

$$\Delta\mathbf{y}(t) = \mathbf{C}_1\Delta\mathbf{x}_1(t). \tag{4.3}$$

$\Delta\mathbf{x}_1(t) = [\Delta p(t) \quad \Delta\mathbf{x}^\top(t)]^\top$ is the augmented state of the system, where $p(t)$ is the state of the integrator. $\emptyset$ denotes a vector of zeros. This approach is useful for the design of the LQTSS (see Fig. H.2 on page 245).

The structure depicted in Fig. 4.3 will be used for analysis of the controller for the remainder. However, results of the simulations will enact true plant parameters as well as deviational ones. This was achieved using SIMULINK [175] and the respective analysis schematic models for the system with or without control can be found in Appendix H. The figure does not include the effect of disturbances at this point, as it does not influence the design procedure directly. The effect of disturbances will be investigated in §4.1.3 and §4.1.4.

4.1.2.3 Dimensions

The first step in the design procedure is to determine a model to design the controller from. This has been accomplished previously for all three types of models (see footnote c). With the system $(\mathbf{A}, \mathbf{b}, \mathbf{C})$ available, the next step requires the designer to increase the system from type 0 to type 1 by adding an integrator in the system. This results in a new augmented system $(\mathbf{A}_1, \mathbf{b}_1, \mathbf{C}_1)$. Note that the dimensions of the state, input and output matrices are $\mathbf{A}_1 \in \mathbb{R}^{39\times39}$, $\mathbf{b}_1 \in \mathbb{R}^{39\times1}$ and $\mathbf{C}_1 \in \mathbb{R}^{38\times39}$ respectively.

4.1.2.4 State weighting matrix

A suitable value for the state weighting matrix $\mathbf{H} \in \mathbb{R}^{38\times39}$ must be determined. Since the matrix is multiplied by the state, and since the desired tracking error will be defined as the difference between desired output and true output, the $\mathbf{H}$ matrix can be chosen to equal the output matrix $\mathbf{C}_1$. This ensures that the outputs of the system are worked into the performance index of Eq. 2.49.

4.1.2.5 Error and control weighting

Selection of the weighting matrices $\mathbf{Q}$ and $\mathbf{R}$ is not a trivial procedure. It is known that there is only one manipulated variable (casting speed) and therefore $\mathbf{R} = r \in \mathbb{R}^{1\times 1}$. It is also known that there are 38 outputs (the thermocouple outputs) and thus $\mathbf{Q} \in \mathbb{R}^{38\times 38}$. The design goal is to achieve temperatures that are close to the desired temperatures set-points so that the occurrence of defects is minimised. Therefore it has been decided that it is equally important for the LQTSS to track each of the outputs, and reject disturbances on each of the outputs equally "strongly". This implies that the diagonal matrix $\mathbf{Q}$ will have all elements equal along the main diagonal. This can be expressed mathematically as follows.

$$\mathbf{Q} = q\mathbf{I}_{38}, \tag{4.4}$$

where q is a scalar value indicating the global weight of the tracking error. For constant r values, increasing q improve the performance of the tracker but also increases the required control action. Increasing r with constant q reduces the performance on the tracking error but also reduces the control action. From this, it is interesting to note that the ratio q/r is more useful in determining an optimal value for q, irrespective of the value for r.

Setting about to design a suitable value for q, the designer is not only interested in the improved performance of the system but also the required control action. In this design, the control action is performed by the casting speed, $u(t) = u_1(t)$. Now, the casting speed cannot be too high, with acceptable limits ranging between 600 to 1500 mm/min. Furthermore, the acceleration of the slab can also not be too extreme, with a typical allowable value of $du_1(t)/dt\,|_{max} = 1000\,\text{mm/min}^2$ (slew-rate limitation). The controller design will thus be based of observations of increased performance on the tracking error and constraints imposed on the control action.

With the values for all the weighting matrices known, the designer can proceed to solve the ARE (Eq. 2.50) for $\mathbf{S}_\infty$. With $\mathbf{S}_\infty$ known, the designer can find the feed-forward and state feedback gains from Eqs. 2.51 and 2.48 respectively. Once the gains are known, the controller can be simulated to test the improvement of the system. This was done using SIMULINK (see Figs. H.1 and H.2). If the improvement is unsatisfactory, the ratio q/r can be increased and if the control action is too severe, *i.e.* the casting speed or acceleration is too high, the ratio can be decreased until an optimal point is achieved.

4.1.2.6 q/r ratio

Several different values of the q/r ratio were tested in simulation as depicted in Table 4.1 for 1060mm wide slabs. The SMSMSE[e] value is a mean square error approach to evaluate

Table 4.1 1060mm wide slab errors, maximum acceleration and maximum speeds for the LQTSS implementation at different values of the q/r ratio.

$\frac{q}{r}$	SMSMSE	$\max\lvert du_1/dt\rvert$	$\max(u_1)$
None	5.199	0	955.8
0.001	4.5915	22.48	1075
0.01	4.1619	60.3	1120
0.1	3.8945	135.6	1155
1	3.7586	272.2	1180
10	3.6945	517.8	1196
100	3.6644	957	1206
1000	3.6498	1754	1212
10000	3.6424	2992	1215
115	3.6632	997.9	1206

the overall error between the desired set-points of the temperatures and the temperatures themselves. It is defined for this thesis as $\text{SMSMSE} = \sqrt{\text{MSMSE}}$, where

$$\text{MSMSE} = \frac{1}{38}\sum_{j=1}^{38}\text{MSE}_j. \tag{4.5}$$

$\text{MSE} \in \mathbb{R}^{1\times 38}$ is the mean square error between each of the temperature outputs and their respective set-points[f] defined by

$$\text{MSE}_j = \frac{1}{N}\sum_{i=1}^{N}\left(r_j[i] - y_j[i]\right)^2. \tag{4.6}$$

N is the number of time samples used to calculate the MSE. $r_j[i]$ denotes the i-th sample of the j-th set-point and $y_j[i]$ denotes the i-th sample of the j-th output. $\max|du_1/dt|$ is the maximum acceleration of casting speed which should remain below 1000mm/min^2, and $\max(u_1)$ is the maximum value of the casting speed (typically less than 1500 mm/min).

The first row in Table 4.1 denotes the different evaluation parameters when no control is used *i.e.* open-loop. They were derived by using the optimal casting speed[g] as the input to the system and typical mould level and water temperature as disturbances. For this reason,

[e] Square-root of the Mean Sum of Mean Square Errors

[f] see Eq.2.39

[g] the optimal casting speed is calculated using the optimal thermocouple temperature set-points in an inversion with the MVIV model. For the 1060mm case, this optimal speed is 955mm/min.

the acceleration of the slab remains zero (casting speed is constant). Several q/r ratios were used to design controllers in the form of the $\mathbf{F}(\infty)$ and $\mathbf{K}_\infty$ gains. As can be seen, a controller designed with a q/r ratio of 0.001 improved the overall SMSMSE by approximately 12%. As the ratio is increased, the SMSMSE decreases, implying greater control action in the form of greater acceleration as well as improved set-point tracking. At the point where the ratio is 115, the acceleration of the slab has reached its maximum allowable value of 1000mm/min. This is also graphically depicted in Fig. 4.4. The value of 115 for the ratio is therefore the

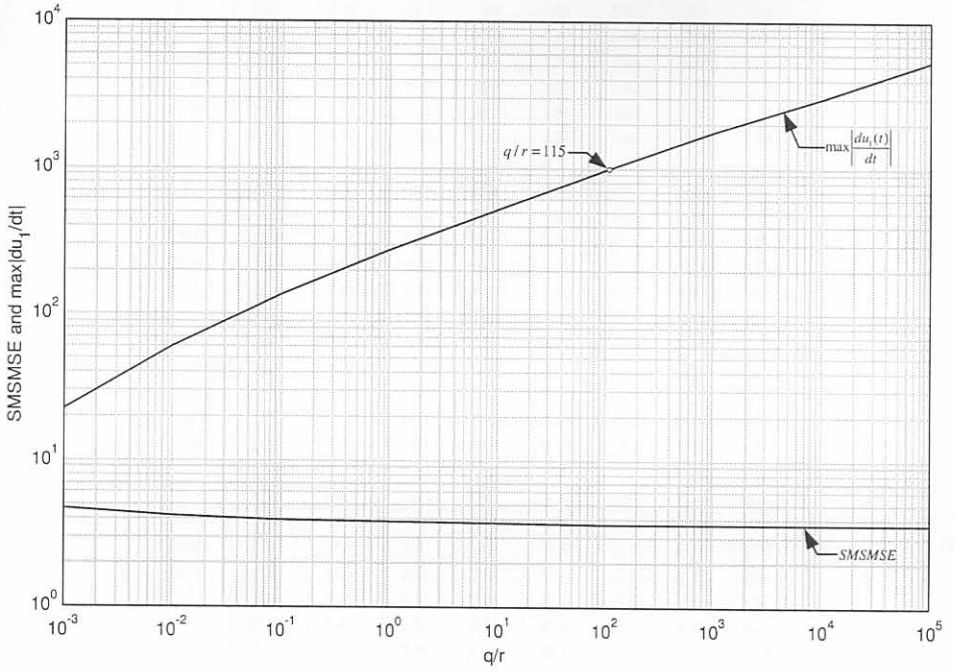

Figure 4.4 SMSMSE and maximum absolute acceleration [mm/min^2] versus q/r ratio for 1060mm slabs.

optimal choice given the model and constraints. At $q/r = 115$, the SMSMSE has improved over the value for no control by approximately 30%.

Inspections of the individual MSE (*i.e.* the effect of the controller on the error of individual set-points) with varying q/r ratios is displayed in Table 4.2. The table shows that some MSEs have been improved dramatically (*e.g.* in5u and in6l) while some have deteriorated (*e.g.* in2u). This is due to the averaging out characteristic of the LQTSS. Overall, an improvement is achieved by looking at the SMSMSE.

Table 4.2 Mean Square Errors for the LQTSS implementation for 1060mm wide slabs at different values of the q/r ratio. $q/r = 115$ has the maximum acceleration of 1000mm/min^2.

$\frac{q}{r}$	in1u	in1l	in2u	in2l	in3u	in3l	in4u	in4l
None	10.7	42.6	10.6	12	2.2	0.569	42.5	21.2
0.001	6.23	27.7	12.8	15	1.38	2.31	33.1	13.1
0.01	3.08	17.3	14.4	17.1	0.969	3.94	26.3	8
0.1	1.78	10.8	15.6	18.7	1.16	5.38	21.7	4.94
1	1.62	7.36	16.4	19.8	1.58	6.46	18.9	3.31
10	1.87	5.53	16.9	20.5	1.97	7.18	17.3	2.45
100	2.16	4.57	17.2	20.9	2.25	7.64	16.4	2
1000	2.38	4.04	17.3	21.1	2.44	7.92	15.9	1.76
10000	2.53	3.75	17.5	21.3	2.56	8.08	15.6	1.62
115	2.17	4.52	17.2	20.9	2.27	7.66	16.3	1.98

$\frac{q}{r}$	in5u	in5l	in6u	in6l	in7u	in7l	in8u	in8l
None	1.63	21.8	15.9	107	6.49	58.6	1.44	43.9
0.001	1.19	14	10.2	76.4	3.64	41.4	1.16	33.1
0.01	0.889	8.55	5.69	56.9	1.67	29.5	1.24	24.4
0.1	0.963	5.21	2.93	44.1	0.741	21.7	1.78	18.5
1	1.2	3.44	1.54	36.6	0.467	17.2	2.44	15.1
10	1.44	2.51	0.893	32.3	0.45	14.7	2.98	13.2
100	1.62	2.03	0.592	29.8	0.5	13.3	3.36	12.1
1000	1.74	1.77	0.447	28.5	0.552	12.5	3.61	11.5
10000	1.82	1.63	0.373	27.7	0.589	12.1	3.76	11.1
115	1.63	2.01	0.58	29.7	0.504	13.2	3.38	12

$\frac{q}{r}$	ou1u	ou1l	ou2u	ou2l	ou3u	ou3l	ou4u	ou4l
None	0.235	32.5	7.21	24.5	21.4	1.79	1.65	6.85
0.001	5.19	21.5	3.9	14.1	29.2	7.54	4.18	9.76
0.01	10.6	13.3	2.14	7.35	35.4	12.3	6.15	11.6
0.1	15.8	8.15	1.99	3.56	40.1	16.5	7.81	13.1
1	20	5.41	2.6	1.78	43.4	19.6	9.01	14
10	22.9	3.99	3.28	1	45.5	21.7	9.81	14.7
100	24.7	3.25	3.82	0.651	46.7	23	10.3	15.1
1000	25.8	2.85	4.18	0.488	47.5	23.8	10.6	15.3
10000	26.5	2.63	4.41	0.409	47.9	24.3	10.8	15.4
115	24.8	3.22	3.84	0.637	46.8	23.1	10.3	15.1

$\frac{q}{r}$	ou5u	ou5l	ou6u	ou6l	ou7u	ou7l	ou8u	ou8l
None	22.3	61	NA	NA	81.2	213	3.01	98
0.001	16	43.4	NA	NA	58.6	164	3.13	71.1
0.01	11	31.3	NA	NA	42.6	140	4.46	51
0.1	7.77	23.4	NA	NA	32.1	123	6.89	37.7
1	5.92	18.8	NA	NA	26	112	9.32	30
10	4.9	16.2	NA	NA	22.5	106	11.2	25.7
100	4.35	14.8	NA	NA	20.6	102	12.5	23.3
1000	4.04	14	NA	NA	19.5	100	13.3	22
10000	3.86	13.5	NA	NA	18.9	98.9	13.8	21.2
115	4.32	14.7	NA	NA	20.5	102	12.6	23.2

$\frac{q}{r}$	nl1u	nl1l	nl2u	nl2l	nr1u	nr1l	nr2u	nr2l
None	1.25	0.0794	0.233	17.7	2.11	21.9	8.12	1.77
0.001	0.749	0.267	0.843	22.7	1.42	17.8	10.4	2.34
0.01	0.37	0.51	1.32	27.1	0.785	14.3	12.4	2.85
0.1	0.173	0.744	1.77	30.6	0.477	11.9	14	3.25
1	0.103	0.926	2.12	33	0.385	10.4	15.1	3.53
10	0.0906	1.05	2.36	34.5	0.382	9.58	15.7	3.7
100	0.0957	1.13	2.51	35.4	0.401	9.1	16.1	3.8
1000	0.104	1.18	2.61	35.9	0.421	8.82	16.4	3.86
10000	0.11	1.21	2.66	36.2	0.434	8.66	16.5	3.9
115	0.0962	1.13	2.52	35.4	0.403	9.08	16.2	3.81

4.1.2.7 Feed-forward and feedback gains

The selected design ratio of 115 resulted in the feed-forward and feedback gain vectors depicted in tables 4.3 and 4.4.

Table 4.3 Feed-forward gain matrix $\mathbf{F}(\infty)$ for 1060mm wide slabs at $q/r = 115$.

in1u	in1l	in2u	in2l	in3u	in3l	in4u	in4l
2.12	2.36	0.505	0.658	1.42	1.12	1.38	1.93
in5u	in5l	in6u	in6l	in7u	in7l	in8u	in8l
1.09	1.78	1.64	2.88	1.51	2.21	1.39	1.6
ou1u	ou1l	ou2u	ou2l	ou3u	ou3l	ou4u	ou4l
2.25	2.07	2.24	2.41	1.22	2.12	1.06	0.842
ou5u	ou5l	ou6u	ou6l	ou7u	ou7l	ou8u	ou8l
1.34	2.24	NA	NA	2.48	3.37	2.38	2.64
nl1u	nl1l	nl2u	nl2l	nr1u	nr1l	nr2u	nr2l
0.621	0.467	0.601	0.851	0.798	0.817	0.56	0.304

Table 4.4 Feedback gain matrix $\mathbf{K}_\infty$ for 1060mm wide slabs at $q/r = 115$. The gain of the integrator state is $k_\infty = 0.230$.

in1u	in1l	in2u	in2l	in3u	in3l	in4u	in4l
2.84	2.07	0.388	0.486	1.5	0.928	1.11	1.44
in5u	in5l	in6u	in6l	in7u	in7l	in8u	in8l
2.79	1.51	2.01	2.16	1.54	1.81	1.83	1.59
ou1u	ou1l	ou2u	ou2l	ou3u	ou3l	ou4u	ou4l
2.54	1.9	2.21	2.02	0.987	1.55	0.851	0.573
ou5u	ou5l	ou6u	ou6l	ou7u	ou7l	ou8u	ou8l
1.32	1.78	NA	NA	2.02	2.14	3.26	2.4
nl1u	nl1l	nl2u	nl2l	nr1u	nr1l	nr2u	nr2l
0.879	0.562	0.622	0.897	1.07	0.892	0.633	0.317

Narrow side gains are on the whole less than wide side gains, specifically for the following two reasons.

- Temperature control is easier to achieve on the narrow sides than the wide sides because the water flow in the copper mould at the narrow sides is approximately 4 times less than at the wide sides. In contrast the wide side is less than 4 times wider than the narrow side. This results in proportionally more water flow in the narrow side which ensures more cooling so that temperature variation is more dramatic when casting speed changes.
- Surface defects on the wide sides were included in the study and not on the narrow sides. This implies that the narrow sides in effect do not affect the design procedure as

much as the wide sides. Care should be taken however that the narrow side-wide side temperature gradient could have an effect on the defects, and can thus not be excluded from the model or the design.

4.1.3 Time-domain results

The following set of figures indicates the effect of the controllers on the system in the time domain. These figures were generated using simulation of the system model with and without controllers. Standard practical disturbances were included to investigate the effectiveness of the controllers. 1060mm wide slabs will be used to discuss the time-domain results and 1280mm wide and 1575mm wide slab results can be found in appendix H.

Fig. 4.5 shows the practical mould level disturbance and Fig. 4.6 shows the practical water temperature disturbance for the controller synthesis for 1060mm wide slabs. The sharp decrease in the mould level at $t \approx 160000$ seconds is probably due to manual mould level control. Fig. 4.7 shows the output of the system when the optimal static control value is

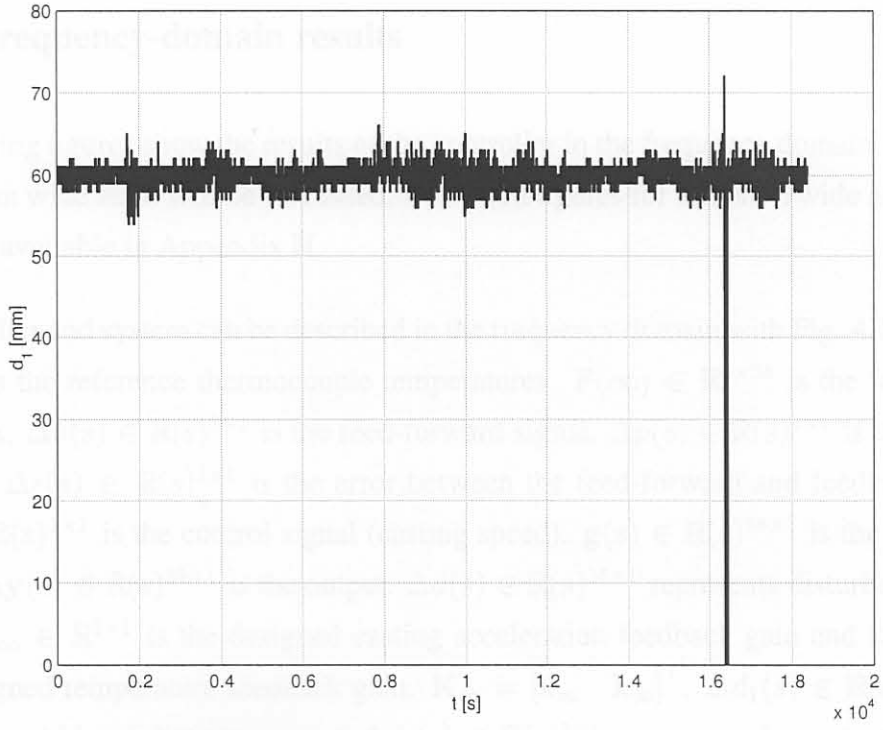

Figure 4.5 Mould level disturbance ($d_1(t)$) used for the simulation of the 1060mm wide slab system.

applied, and Fig. 4.8 shows the outputs when the LQTSS controller is used with 1060mm

wide slabs. The q/r ratio is 115. The figures show that there has been a reduction in the variability of the temperatures. This becomes more evident when looking at the error between the reference output and true output. Figures 4.9 and 4.10 show the errors with and without control. A reduction of about 10°C has been achieved in peak changes of temperature tracking errors when the LQTSS has been used. The set-points are not being followed perfectly, and a reduction in the number of defects of only 18% is achieved. This value was calculated using the IVOV model, and simulating the thermocouple temperatures with, and without the controller implementation. The value is conservative, because it is based on a simulation with the IVOV model predictor. The small reduction in the occurrence of defects is probably due to the fact that good control is difficult to achieve since there are so many outputs which have to be controlled.

Figure 4.11 shows the control signal (casting speed), and Fig. 4.12 the acceleration of the slab for the LQTSS implementation. The speed graph shows that the maximum actuator output constraint (1500mm/min) has not been violated and the acceleration graph shows that the maximum absolute acceleration is less than 1000mm/min^2.

4.1.4 Frequency-domain results

The following figures show the results of the controller in the frequency domain. The figures for 1060mm wide slabs will be discussed, with extra figures for 1280mm wide and 1575mm wide slabs available in Appendix H.

The controller and system can be described in the frequency domain with Fig. 4.13. $\Delta\mathbf{r}(s) \in \mathbb{R}(s)^{38\times1}$ is the reference thermocouple temperatures. $\mathbf{F}(\infty) \in \mathbb{R}^{1\times38}$ is the feed-forward gain matrix. $\Delta v(s) \in \mathbb{R}(s)^{1\times1}$ is the feed-forward signal. $\Delta p(s) \in \mathbb{R}(s)^{1\times1}$ is the feedback signal and $\Delta\epsilon(s) \in \mathbb{R}(s)^{1\times1}$ is the error between the feed-forward and feedback signals. $\Delta u(s) \in \mathbb{R}(s)^{1\times1}$ is the control signal (casting speed). $\mathbf{g}(s) \in \mathbb{R}(s)^{38\times1}$ is the MVIV system, and $\Delta\mathbf{y}(s) \in \mathbb{R}(s)^{38\times1}$ is the output. $\Delta d(s) \in \mathbb{R}(s)^{38\times1}$ represents disturbances on the outputs. $k_\infty \in \mathbb{R}^{1\times1}$ is the designed casting acceleration feedback gain and $\mathbf{k}_\infty \in \mathbb{R}^{38\times1}$ is the designed temperature feedback gain. $\mathbf{K}_\infty = [k_\infty \quad \mathbf{k}_\infty]^\top$. $\Delta d_1(s) \in \mathbb{R}(s)^{1\times1}$ represents the mould level disturbance and $\Delta d_2(s) \in \mathbb{R}(s)^{1\times1}$ represents the water temperature disturbance. $\mathbf{g}_{d_1}(s) \in \mathbb{R}(s)^{38\times1}$ represents the effect or transfer of the mould level on the temperatures and $\mathbf{g}_{d_2}(s) \in \mathbb{R}(s)^{38\times1}$ represents the effect of the water temperature on the temperatures.

The first two figures (Fig. 4.14 and 4.15) show the double-sided spectrum of the two distur-

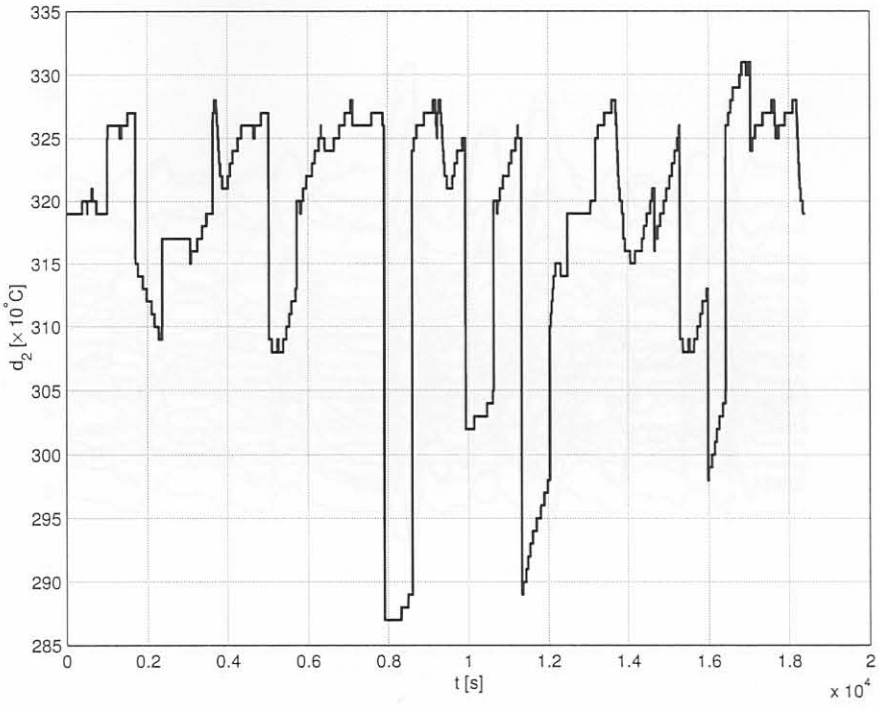

Figure 4.6 Water temperature ($d_2(t)$) disturbance used for the simulation of the 1060mm wide slab system.

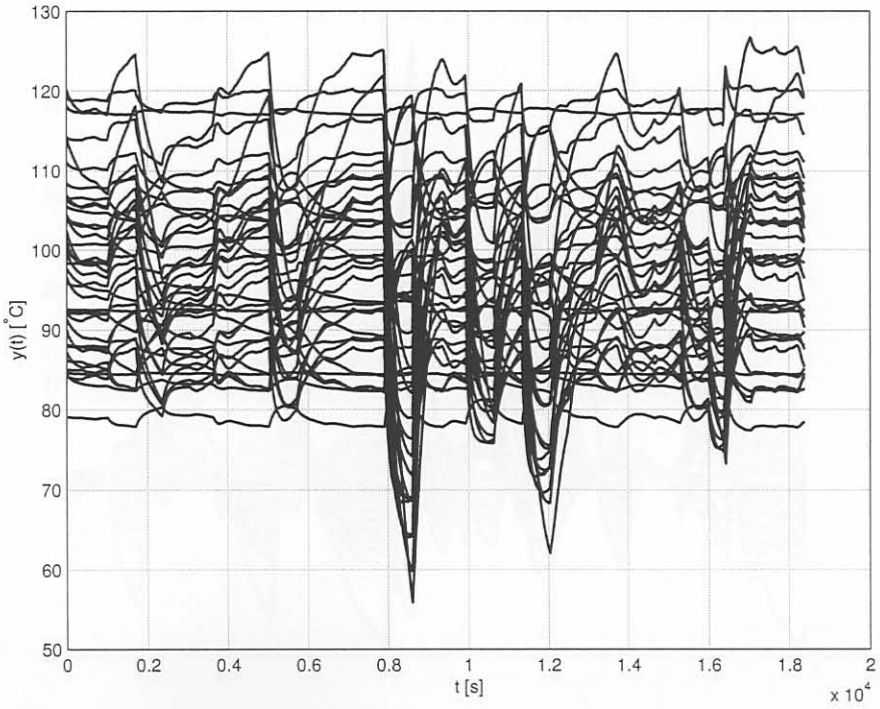

Figure 4.7 Outputs ($\mathbf{y}(t)$) of the system without the LQTSS controller for 1060mm wide slabs.

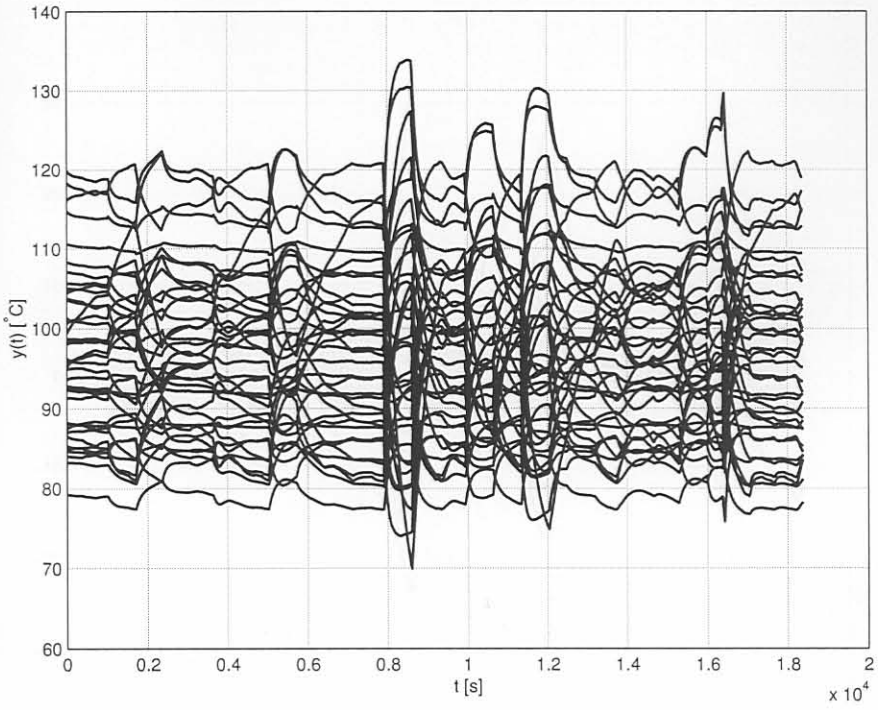

Figure 4.8 Outputs $(\mathbf{y}(t))$ of the system with the LQTSS controller for 1060mm wide slabs.

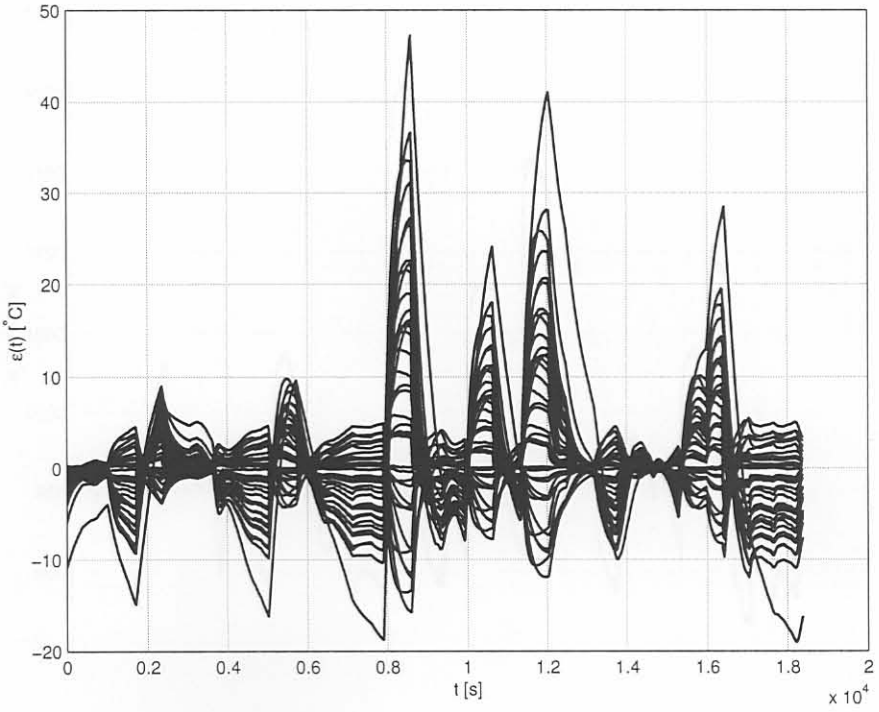

Figure 4.9 Tracking errors of the system without the LQTSS controller for 1060mm wide slabs.

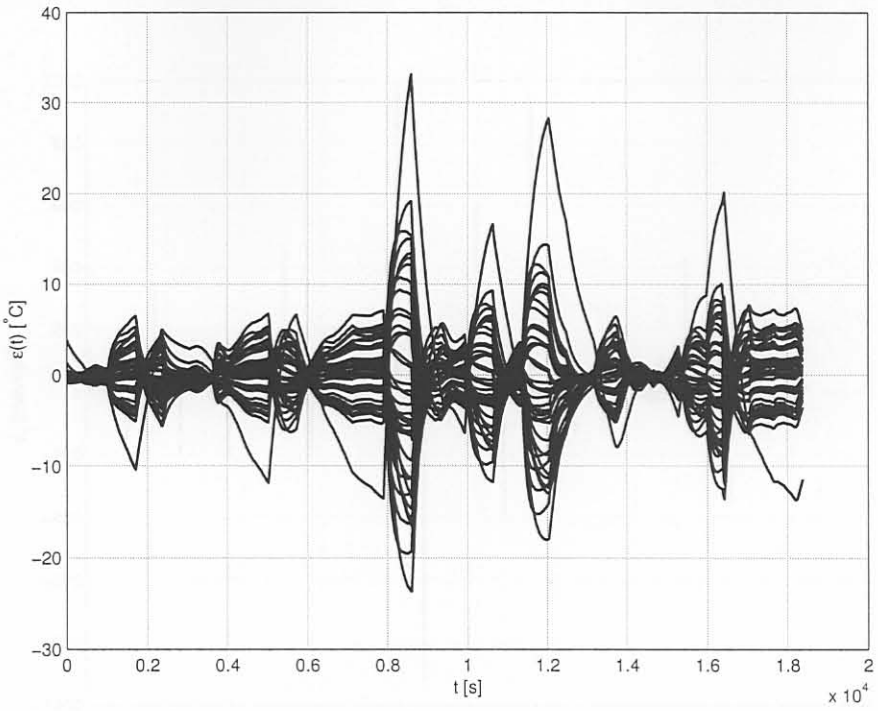

Figure 4.10 Tracking errors of the system with the LQTSS controller for 1060mm wide slabs.

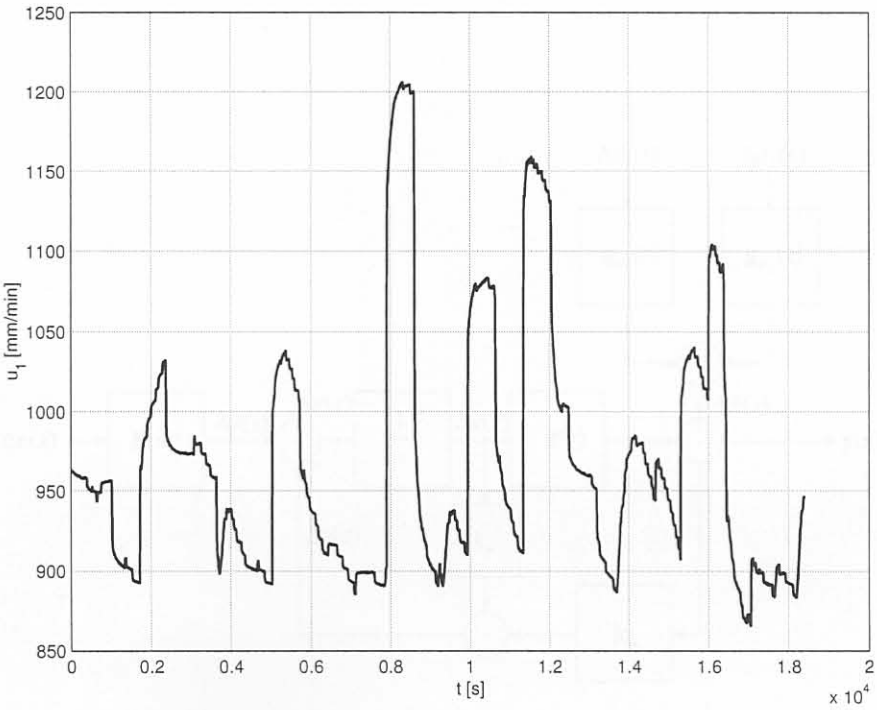

Figure 4.11 Casting speed (casting speed, $u_1(t)$) for the LQTSS controller for 1060mm wide slabs.

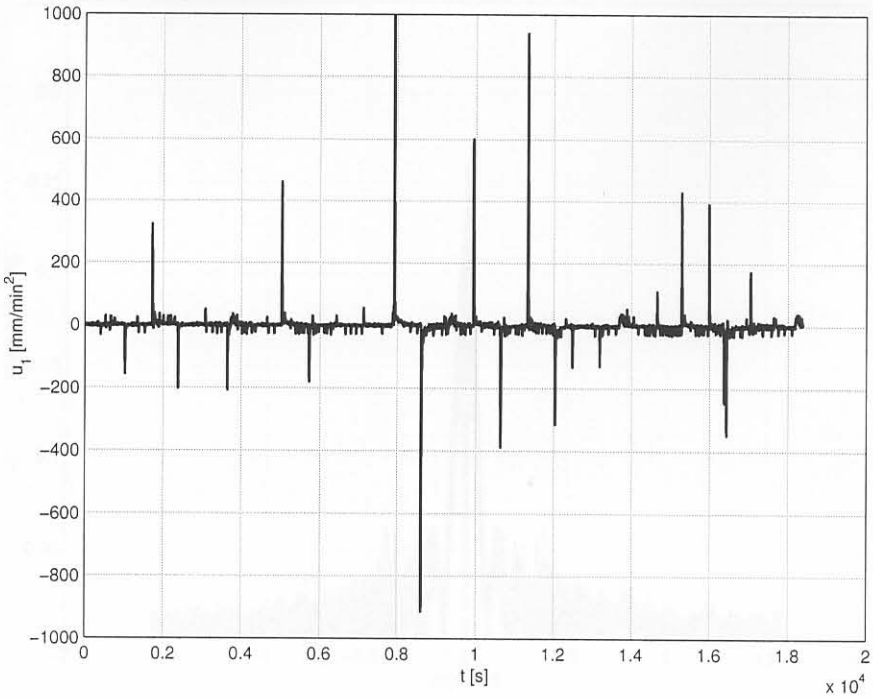

Figure 4.12 Casting acceleration for the LQTSS controller for 1060mm wide slabs.

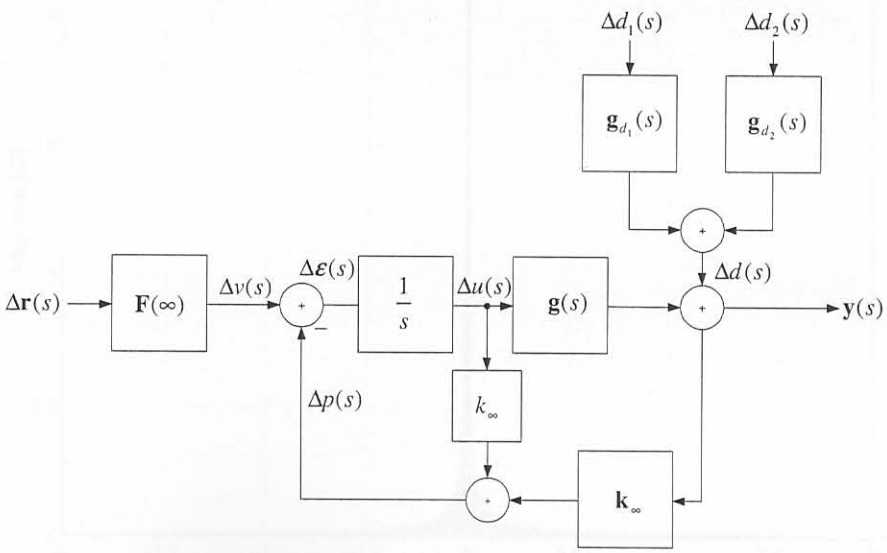

Figure 4.13 Description of the control system in the frequency domain.

bances under investigation, $d_1(j\omega)$ and $d_2(j\omega)$. Fig. 4.16 and Fig. 4.17 show the normalized

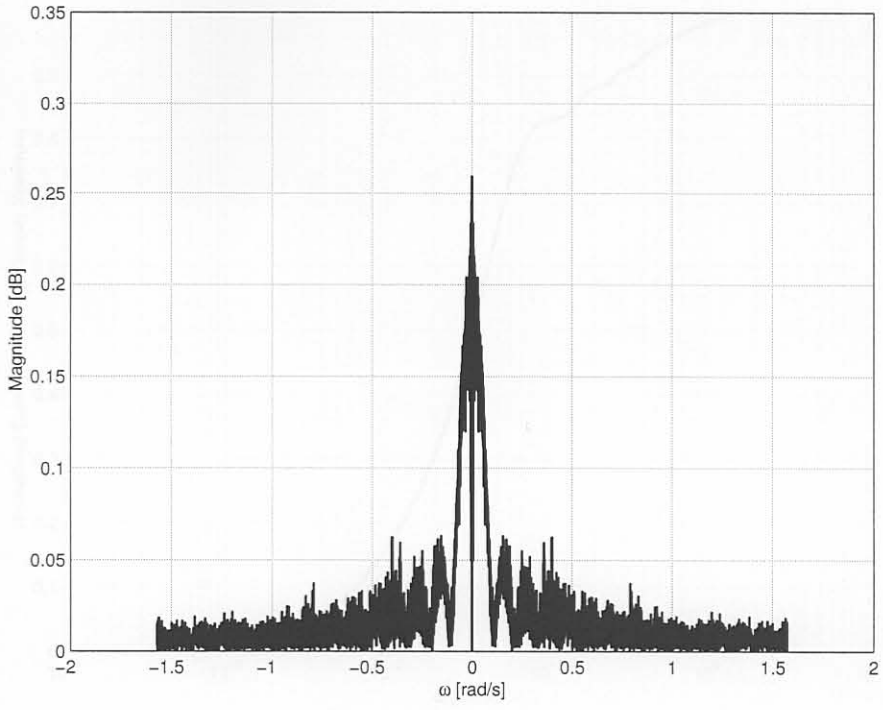

Figure 4.14 Spectrum of mould level disturbance, $d_1(j\omega)$, with average trend removed.

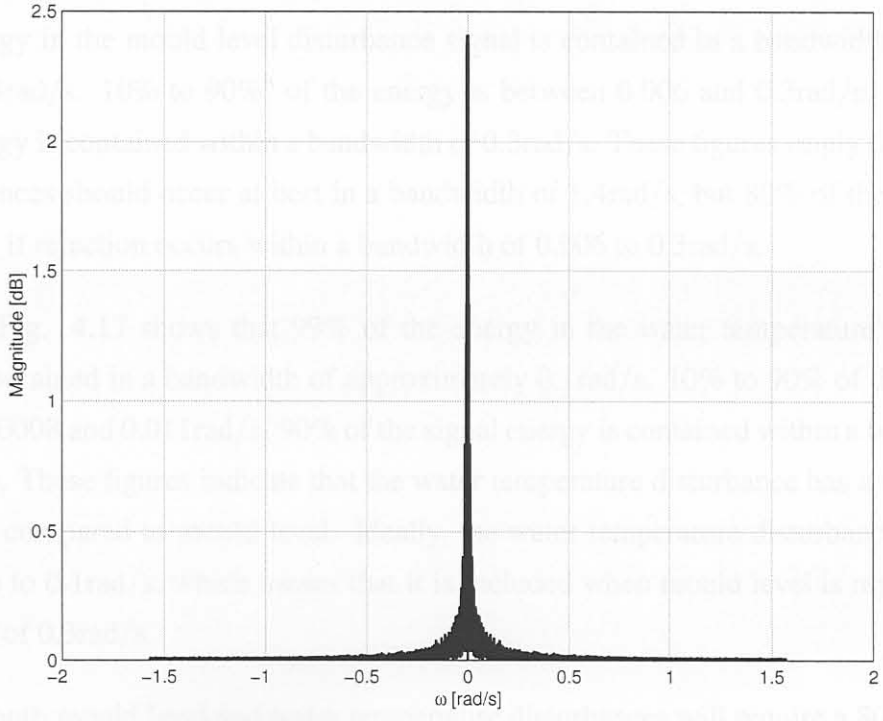

Figure 4.15 Spectrum of water temperature disturbance, $d_2(j\omega)$, with average trend removed.

cumulative energy density spectrum for the two disturbances. Fig. 4.16 shows that 99%

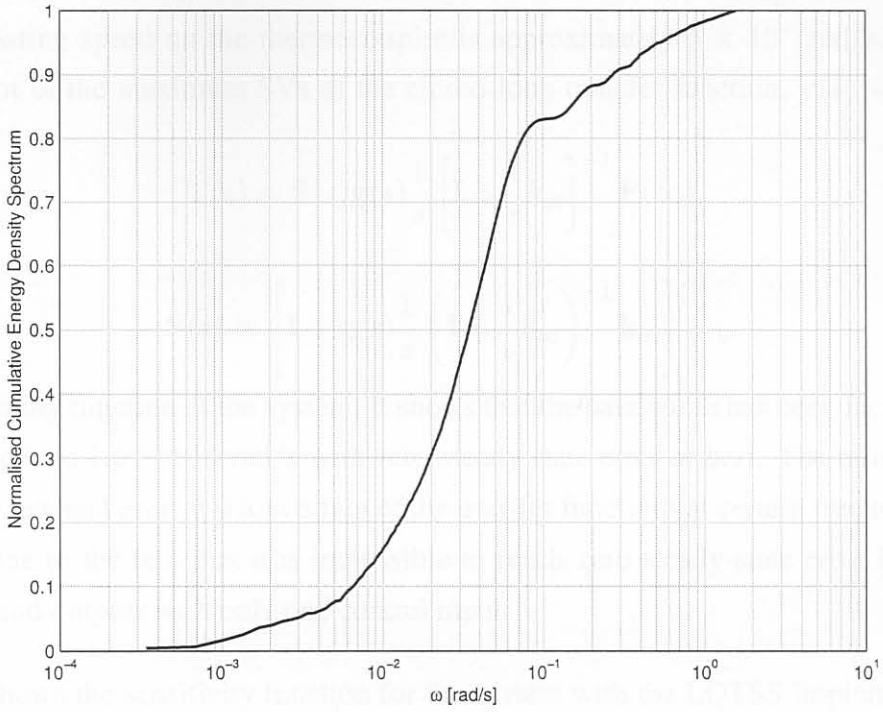

Figure 4.16 Normalized cumulative energy density spectrum for the mould level disturbance

of the energy in the mould level disturbance signal is contained in a bandwidth of approximately 1.4rad/s. 10% to 90%[h] of the energy is between 0.006 and 0.3rad/s. 90% of the signal energy is contained within a bandwidth of 0.3rad/s. These figures imply that rejection of disturbances should occur at best in a bandwidth of 1.4rad/s, but 80% of the energy can be rejected if rejection occurs within a bandwidth of 0.006 to 0.3rad/s.

Similarly, Fig. 4.17 shows that 99% of the energy in the water temperature disturbance signal is contained in a bandwidth of approximately 0.1rad/s. 10% to 90% of the energy is between 0.0008 and 0.011rad/s. 90% of the signal energy is contained within a bandwidth of 0.011rad/s. These figures indicate that the water temperature disturbance has a very narrow bandwidth compared to mould level. Ideally, the water temperature disturbance should be rejected up to 0.1rad/s, which means that it is included when mould level is rejected in the bandwidth of 0.3rad/s.

Rejecting both mould level and water temperature disturbances will require a 80% rejection bandwidth of between 0.0008 and 0.3rad/s.

[h] 80% rejection bandwidth

Fig. 4.18 shows the open-loop SVD plot of the effect of casting speed on the thermocouple temperatures for 1060mm wide slabs. The figure shows that the average bandwidth of the effect of casting speed on the thermocouples is approximately 5×10^{-3}rad/s. Fig. 4.19 shows a plot of the maximum SVs of the closed-loop transfer function, $\mathbf{y}(s) = \mathbf{T}(s)\mathbf{r}(s)$, where

$$\mathbf{T}(s) = \mathbf{S}(s)\mathbf{g}(s)\frac{1}{s}\left[\mathbf{I} + \frac{1}{s}k_\infty\right]^{-1}\mathbf{F}(\infty), \tag{4.7}$$

and

$$\mathbf{S}(s) = \left[\mathbf{I} + \mathbf{g}(s)\frac{1}{s}\left(\mathbf{I} + \frac{1}{s}k_\infty\right)^{-1}\mathbf{k}_\infty\right]^{-1}, \tag{4.8}$$

is the sensitivity function of the system. It shows that the bandwidth has been increased from 5×10^{-3}rad/s to 1.5×10^{-1}rad/s with zero-steady state error *at best*. The minimum SVD can be very low and even at 0 for certain of the transfer functions at certain frequencies. This is mainly due to the fact that it is impossible to reach zero steady-state error between the references and outputs with only one control input.

Fig. 4.20 shows the sensitivity function for the system with the LQTSS implementation. It shows that disturbances acting on the system can be rejected over a range of frequencies up to 1.5×10^{-1}rad/s at best, but could even be amplified at some frequencies in the frequency range. This should be interpreted as an improvement in disturbance rejection on some outputs and a weakening of the disturbance rejection on other.

Figs. 4.21 and 4.22 show the improvement of the addition of control over no control. Even though the sensitivity function showed that there is only disturbance rejection up to approximately 1.5×10^{-1}rad/s, the transfer between the mould level disturbance and the outputs together or without LQTSS control has a -33dB attenuation at 0.3rad/s (the bandwidth of the mould level disturbance) on average. Fig. 4.21 also shows that there is about a 1.5dB improvement in attenuation in the mould level disturbance at low frequencies, decreasing as frequency increases up to about 4×10^{-2}rad/s where the attenuation improvement is marginal.

The water temperature to output temperature transfer function shows that at 0.011rad/s (bandwidth of water temperature disturbance) there is an improvement of about 2.5dB on the attenuation of the disturbance, using the LQTSS. This attenuation improvement increases towards DC. At 8×10^{-4}rad/s there is an improvement in attenuation of about 3dB. At 2×10^{-1}rad/s the attenuation weakens, but is of no concern since this point falls outside the spectrum of the water temperature disturbance.

Fig. 4.23 shows the transfer function defined by $h(s) = p(s)/v(s)$. This is the transfer

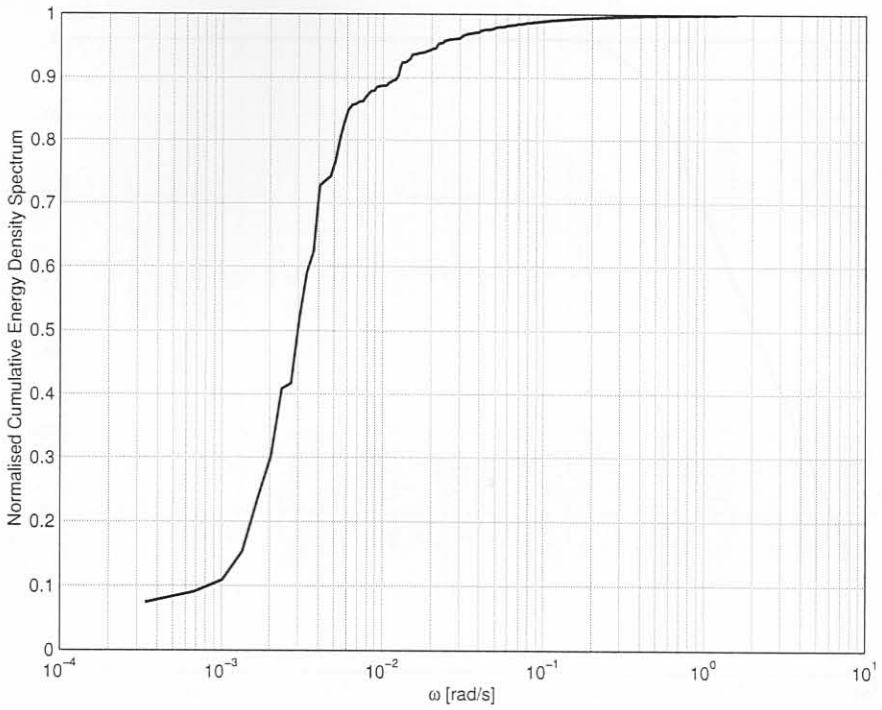

Figure 4.17 Normalized cumulative energy density spectrum for the water temperature disturbance

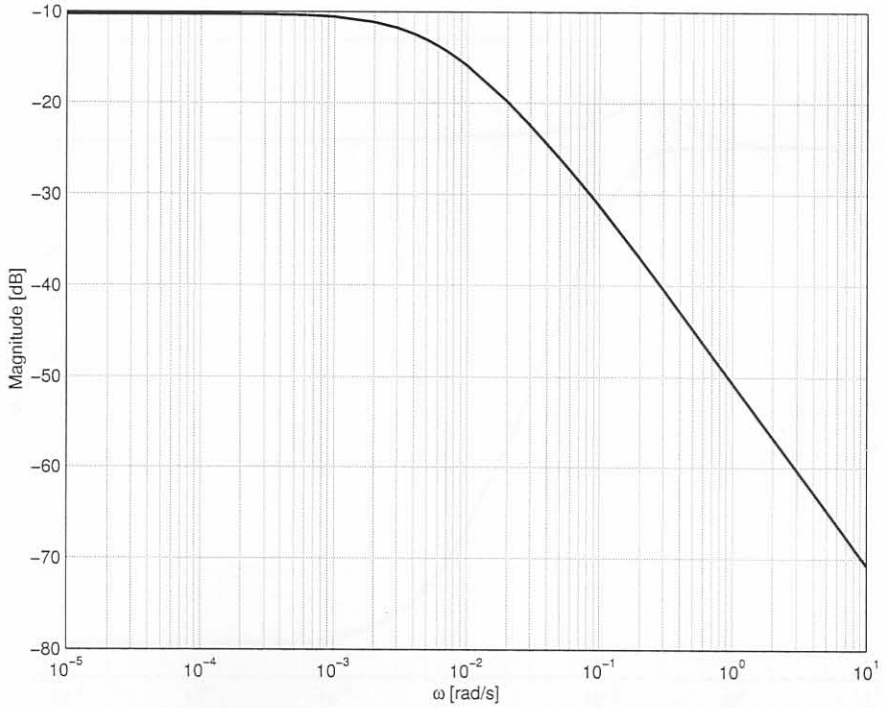

Figure 4.18 Open-loop SVD plot of casting speed to the thermocouple temperatures without control ($\mathbf{g}(s)$).

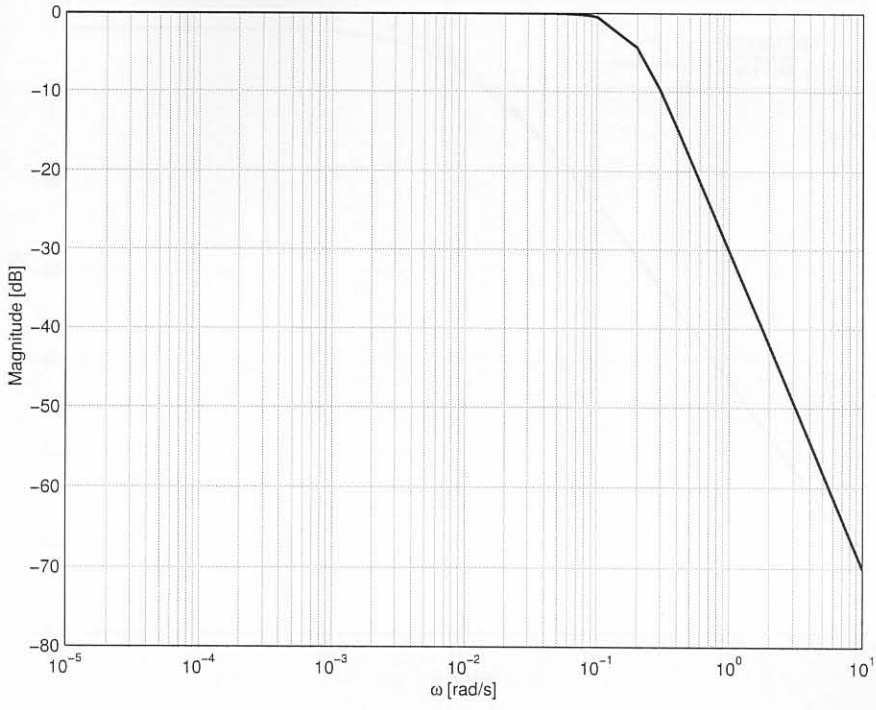

Figure 4.19 Closed-loop maximum SVs plot, $\mathbf{T}(s)$, of the system.

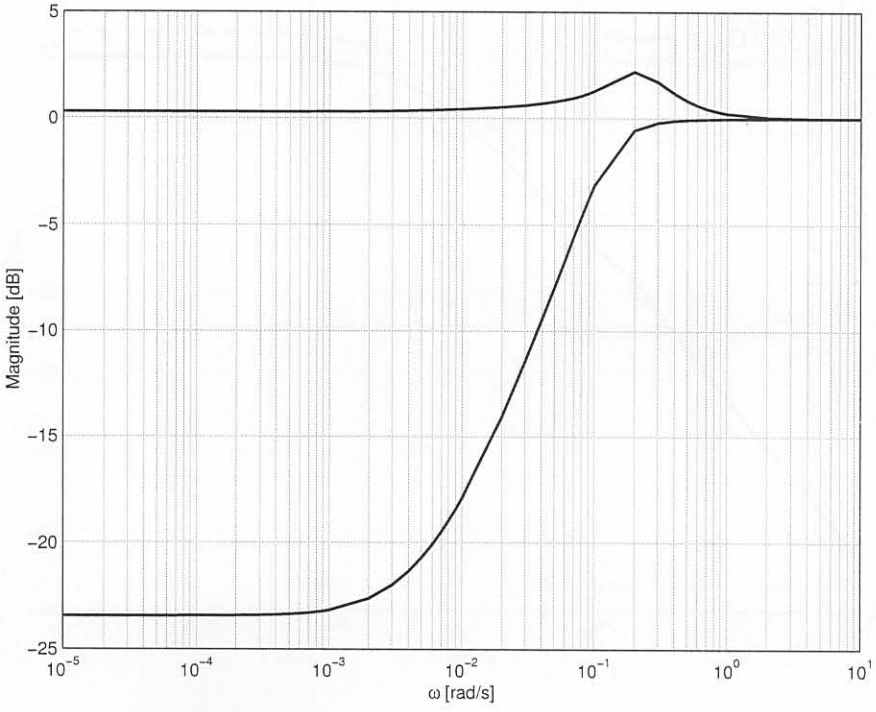

Figure 4.20 Sensitivity function for the system.

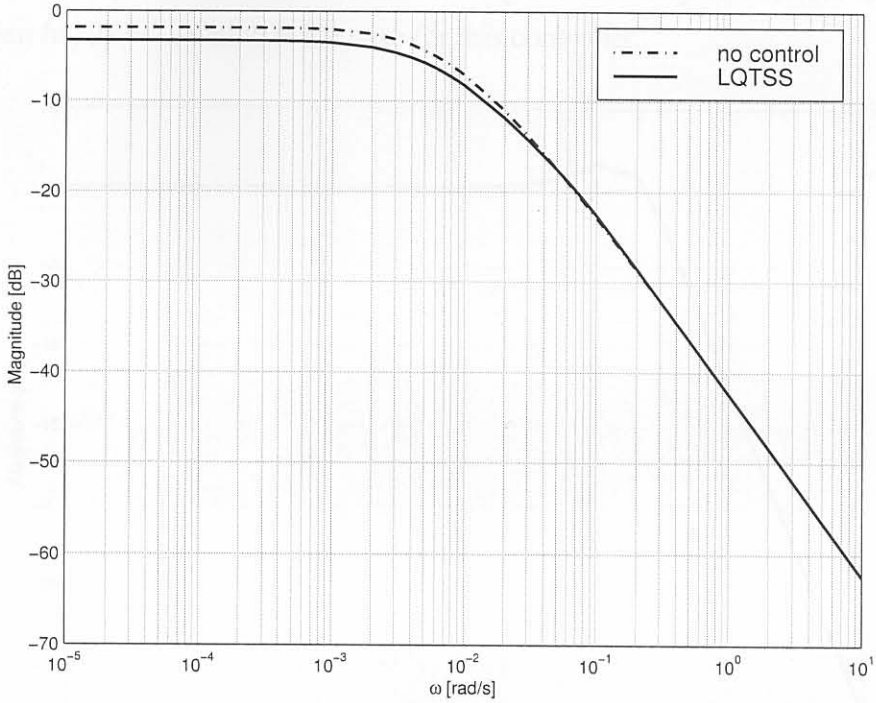

Figure 4.21 Reduction in the effect of mould level disturbance on the output temperatures.

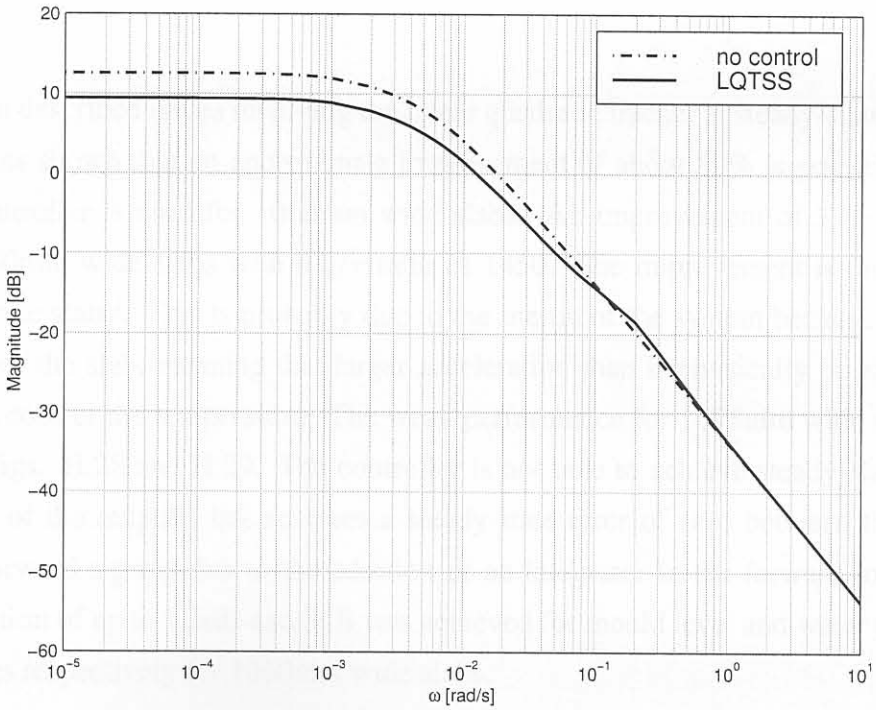

Figure 4.22 Reduction in the effect of water temperature disturbance on the output temperatures.

function between the feed-forward and feedback signals. If steady-state errors for step inputs are zero, then $h(j0) = 1$, which is the case for this controller.

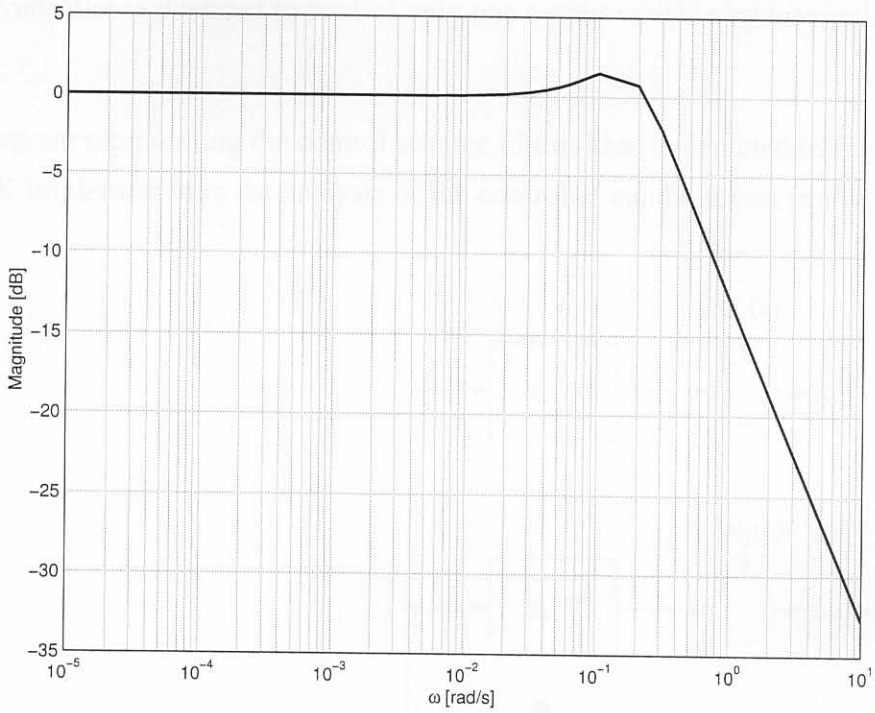

Figure 4.23 Bode plot of the transfer function of $p(s) = h(s)v(s)$.

This section described issues involving the linear quadratic tracker at steady-state implementation. It has shown that an approximate improvement of about 30% is possible when the LQTSS controller is used for 1060mm wide slabs. An improvement of 37% is possible[i] for the 1280mm wide slabs with a q/r ratio of 1450. The improvement is only 0.7% for 1575mm wide slabs[j]. This is probably due to the inertia of the system because of the wide dimension of the slab, meaning that larger acceleration than is physically possible may be required to control the temperature. The weak performance for 1575mm wide slabs is also shown in Figs. H.28 and H.29. The controller is not able to achieve steady-state errors of zero on all of the outputs, but achieves a steady-state error of zero between the feedback and feed-forward signals due to the addition of an integrator in the forward loop. Disturbance rejection of up to 1.5dB and 3dB was achieved for mould level and water temperature disturbances respectively for 1060mm wide slabs.

[i] see Table H.1
[j] see Table H.5

4.2 Single-output control (SOC)

The SOC controller is intended to control only one output variable by manipulating casting speed.

A block diagram representing the control scheme of this kind is depicted in Fig. 4.24, and a SIMULINK implementation for analysis of the controller can be found in Fig. I.1 on page 274.

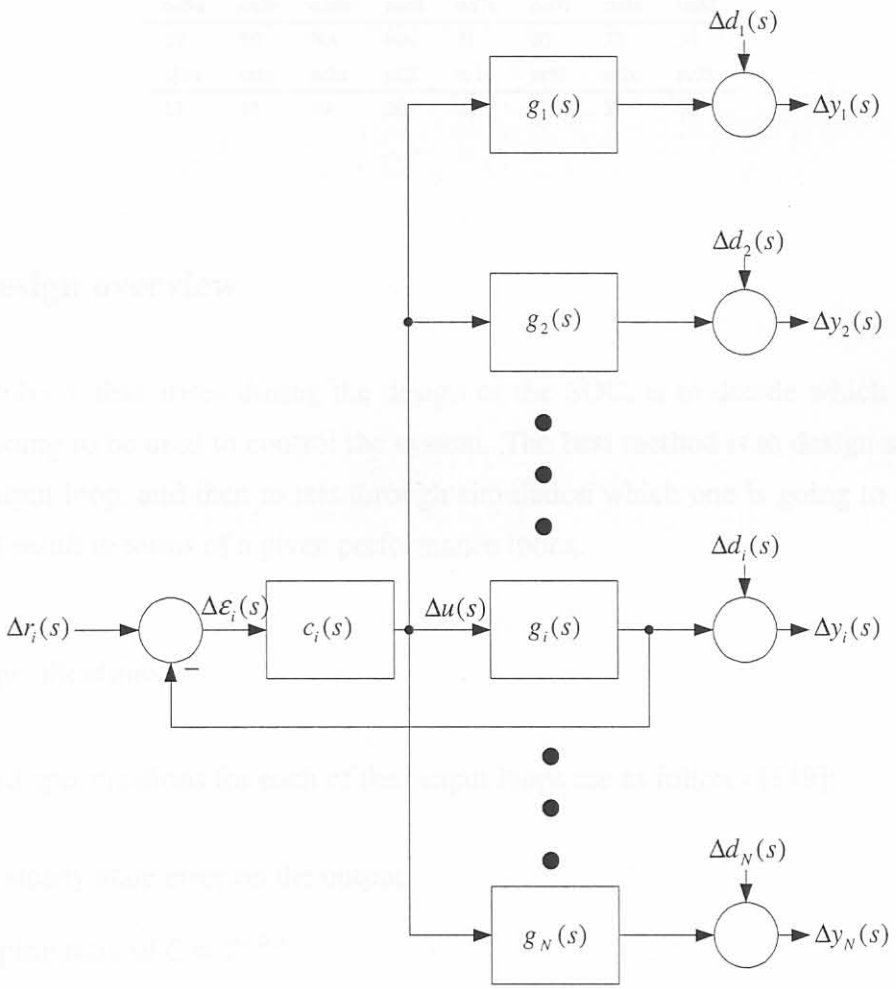

Figure 4.24 Control configuration for the single output control method.

$g_j(s) \in \mathbb{R}(s)^{1\times1}, j = 1, 2, \ldots, N$ denotes the transfer function between casting speed and the j-th thermocouple temperature output ($N = 38$). $\Delta u(s) \in \mathbb{R}(s)^{1\times1}$ is the deviational casting speed, $\Delta y_j(s) \in \mathbb{R}(s)^{1\times1}, j = 1, 2, \ldots, N$ is the j-th deviational thermocouple output and $\Delta d_j(s) \in \mathbb{R}(s)^{1\times1}, j = 1, 2, \ldots, N$ is the j-th deviational disturbance on the j-th output. $\Delta r_i(s) \in \mathbb{R}(s)^{1\times1}$ is the reference set-point for the i-th control loop, and $c_i(s) \in \mathbb{R}(s)^{1\times1}$ is

the controller of the i-th loop. The i-th loop to actual output conversion is given in table 4.5.

Table 4.5 Conversion between loop number, i, and actual output.

in1u	in1l	in2u	in2l	in3u	in3l	in4u	in4l
1	2	3	4	5	6	7	8
in5u	in5l	in6u	in6l	in7u	in7l	in8u	in8l
9	10	11	12	13	14	15	16
ou1u	ou1l	ou2u	ou2l	ou3u	ou3l	ou4u	ou4l
21	22	23	24	25	26	27	28
ou5u	ou5l	ou6u	ou6l	ou7u	ou7l	ou8u	ou8l
29	30	NA	NA	31	32	33	34
nl1u	nl1l	nl2u	nl2l	nr1u	nr1l	nr2u	nr2l
17	18	19	20	35	36	37	38

4.2.1 Design overview

The first problem that arises during the design of the SOC, is to decide which one of the outputs is going to be used to control the system. The best method is to design a controller for each output loop, and then to test through simulation which one is going to deliver the best overall result in terms of a given performance index.

4.2.1.1 Specifications

The standard specifications for each of the output loops are as follows [149]:

1. Zero steady-state error on the output.
2. Damping ratio of $\zeta = 2^{-0.5}$.
3. Maximum bandwidth.
4. Actuator constraints not to be violated.

The design specifications are meant to increase the speed of a loop to a maximum while still maintaining a damping ratio[k] of 0.7071 without breaching the maximum casting speed constraints. The casting speed should remain within about 1500mm/min and the absolute acceleration of the slab (derivative of casting speed) should remain below 1000mm/min^2.

[k]The value chosen for the damping ratio is standard [149], and is the best trade-off between a sluggish response and a large overshoot.

4.2.1.2 PI control

Since the system is of type 0, an integrator must be added in the control loop to increase the system to type 1. This will ensure that the controlled SISO system will have zero steady-state error. A convenient way to design the controllers is to use Evans' root-locus [149], which manipulates a gain in a compensated system. The controller results in a simple PI controller for each i-th loop of the form

$$c_i(s) = k_{i,1} + \frac{k_{i,2}}{s}. \tag{4.9}$$

One zero is placed and one gain is designed to meet the loop specifications [149].

The design process is iterative for each loop, but is simple to carry out, and results in values for $k_{i,1}$ and $k_{i,2}$ for the i-th loop. Eventually, pole-zero plots of the individual loops' closed-loop responses will have a zero to the left of the closed loop poles[1], with the closed loop poles on the $\zeta = 0.7071$ line. This is graphically depicted in Fig. 4.25 for the casting speed to in1u thermocouple system. Following the previous design procedure, the controllers were designed for the 1060mm wide slabs. The results of the values for the proportional and integral gains are given in Tables 4.6 and 4.7.

Table 4.6 1060mm wide slab design values for the proportional gains $k_{i,1}$.

in1u	in1l	in2u	in2l	in3u	in3l	in4u	in4l
226.9	229.9	1874	1510	675.2	1432	447.6	433.9
in5u	in5l	in6u	in6l	in7u	in7l	in8u	in8l
286.5	383.1	290.7	186.4	490.6	249.1	599.1	293.6
ou1u	ou1l	ou2u	ou2l	ou3u	ou3l	ou4u	ou4l
378.3	270	332.7	277.1	607.2	782.2	1351	1601
ou5u	ou5l	ou6u	ou6l	ou7u	ou7l	ou8u	ou8l
419.4	254.8	NA	NA	205.5	201.6	264.8	157.5
nl1u	nl1l	nl2u	nl2l	nr1u	nr1l	nr2u	nr2l
1292	2106	1970	653.9	720.4	620.3	1118	3399

Simulation with each of the respective controllers in the loop delivers the following SMSMSE performance indexes (Table 4.8) for each of the controllers. The table shows that thermocouple output in6u shows the best performance when its controller is used in the loop. Note that this is not better than for the LQTSS 1060mm wide case. Here the MSE was 3.6632, a much better result. This is probably due to the fact that only one loop is used, and all 37 other loops are open. This means that even though near-perfect control can be achieved for one loop, the consequence of not directly controlling all the other loops by leaving them open delivers a worse result than the LQTSS.

[1] the position of the zero is restricted by the actuator constraints

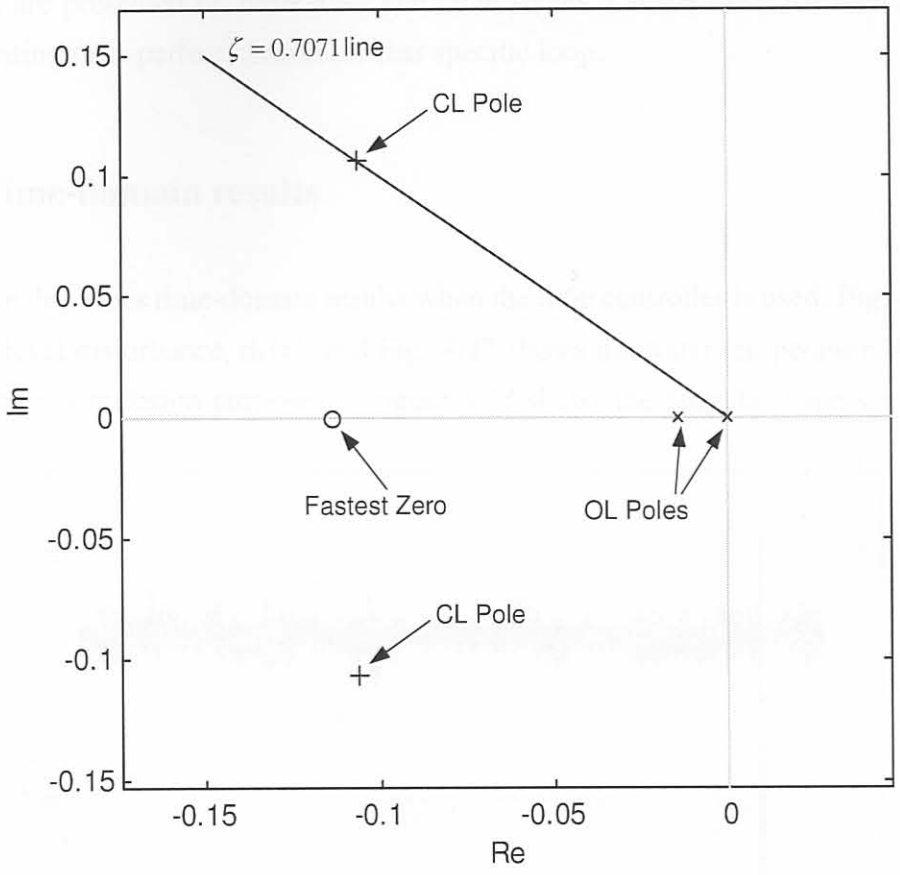

Figure 4.25 Poles and zeros of the open-loop and closed-loop system for 1060mm slabs and the casting speed to in1u thermocouple system. The fastest zero is chosen so that the maximum casting speed constraints are not violated.

Table 4.7 1060mm wide slab design values for the integral gains $k_{i,2}$.

in1u	in1l	in2u	in2l	in3u	in3l	in4u	in4l
25.92	10.9	98.9	73.04	85.17	155.9	18.79	18.49
in5u	in5l	in6u	in6l	in7u	in7l	in8u	in8l
93.75	20.1	27.31	5.463	45.18	9.841	107.4	16.88
ou1u	ou1l	ou2u	ou2l	ou3u	ou3l	ou4u	ou4l
49.71	14.75	28.46	13.95	30.02	59.69	120.6	75.04
ou5u	ou5l	ou6u	ou6l	ou7u	ou7l	ou8u	ou8l
27.84	9.478	NA	NA	7.507	3.582	40.32	6.539
nl1u	nl1l	nl2u	nl2l	nr1u	nr1l	nr2u	nr2l
261.7	366	289.3	50.26	96.14	47.63	111.9	447

Using the thermocouple output in6u loop for control, the MSEs were obtained for each output and are presented in Table 4.9. The table shows that the MSE for in6u is virtually zero, indicating near-perfect control for that specific loop.

4.2.2 Time-domain results

This section describes time-domain results when the in6u controller is used. Fig. 4.26 shows the mould level disturbance, $d_1(t)$, and Fig. 4.27 shows the water temperature disturbance, $d_2(t)$, used for simulation purposes. Figure 4.28 shows the outputs of the system for the

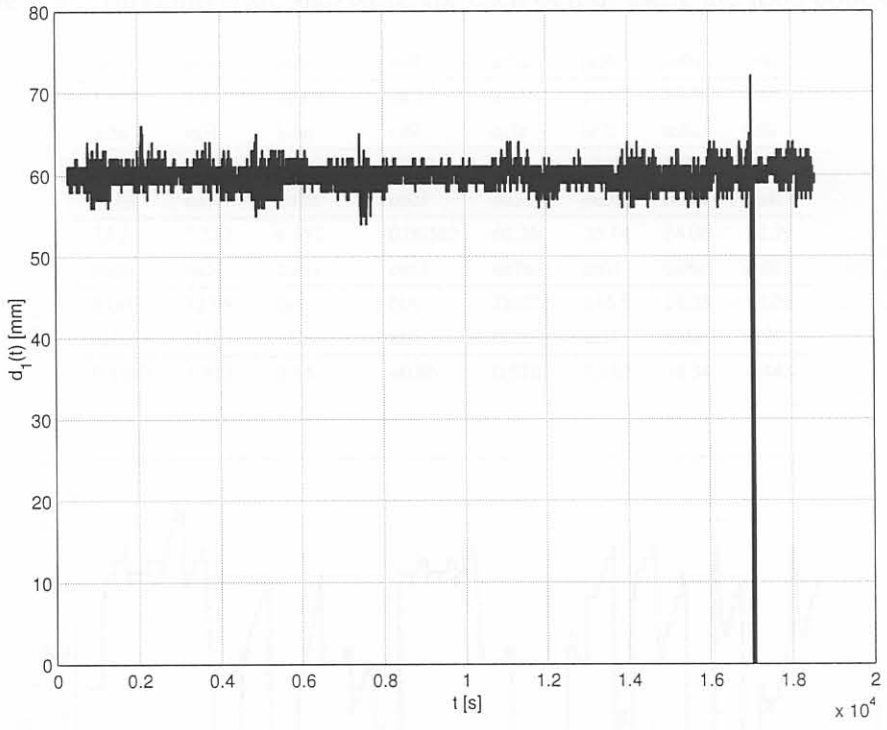

Figure 4.26 Mould level disturbance for the simulation with SOC for 1060mm wide slabs.

SOC control. As can be seen, one of the outputs remains near constant at the temperature set-point, while other temperatures vary. This output is thermocouple in6u. Fig. 4.29 shows the errors between the reference output temperatures and the achieved output temperatures. The result is very similar to that of the LQTSS case, but the peak responses are higher than in the LQTSS case. The casting speed (control signal) and the acceleration of the slab is shown in Figs. 4.30 and 4.31 The acceleration constraint is breached only in two cases at time $t = 3000$ and $t = 11000$ seconds approximately. The control approximately follows the inverse of the water temperature, because this disturbance has the greatest effect on the output temperature (compared to the mould level disturbance).

Table 4.8 1060mm wide slab SMSMSE for each controller in the loop.

in1u	in1l	in2u	in2l	in3u	in3l	in4u	in4l
4.362	4.121	17.6	15.83	4.678	6.684	6.448	4.109
in5u	in5l	**in6u**	in6l	in7u	in7l	in8u	in8l
4.69	4.088	**4.027**	5.184	4.224	4.713	4.881	5.049
ou1u	ou1l	ou2u	ou2l	ou3u	ou3l	ou4u	ou4l
5.913	4.103	4.539	4.036	12.16	6.784	7.627	12.19
ou5u	ou5l	ou6u	ou6l	ou7u	ou7l	ou8u	ou8l
4.468	4.837	NA	NA	4.924	8.875	5.042	4.761
nl1u	nl1l	nl2u	nl2l	nr1u	nr1l	nr2u	nr2l
4.225	5.968	6.447	13.1	4.326	6.791	13.17	12.22

Table 4.9 1060mm wide slab MSE for each output using the in6u controller.

in1u	in1l	in2u	in2l	in3u	in3l	in4u	in4l
3.989	2.21	22.05	28.33	3.635	10.87	16.54	1.15
in5u	in5l	in6u	in6l	in7u	in7l	in8u	in8l
2.601	0.9246	0.002515	28.82	1.01	11.07	5.093	9.854
ou1u	ou1l	ou2u	ou2l	ou3u	ou3l	ou4u	ou4l
33.2	1.532	6.657	0.06362	60.36	35.14	14.06	22.39
ou5u	ou5l	ou6u	ou6l	ou7u	ou7l	ou8u	ou8l
3.007	12.99	NA	NA	18.07	146.9	18.35	18.26
nl1u	nl1l	nl2u	nl2l	nr1u	nr1l	nr2u	nr2l
0.1863	1.513	3.15	40.86	0.5765	8.162	18.34	4.443

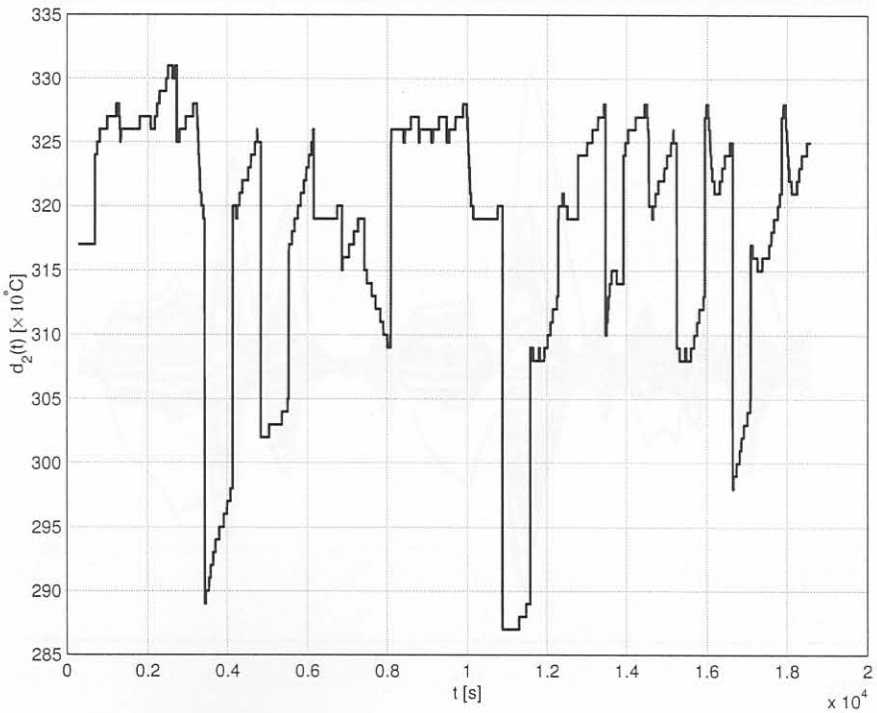

Figure 4.27 Water temperature disturbance for the simulation with SOC for 1060mm wide slabs.

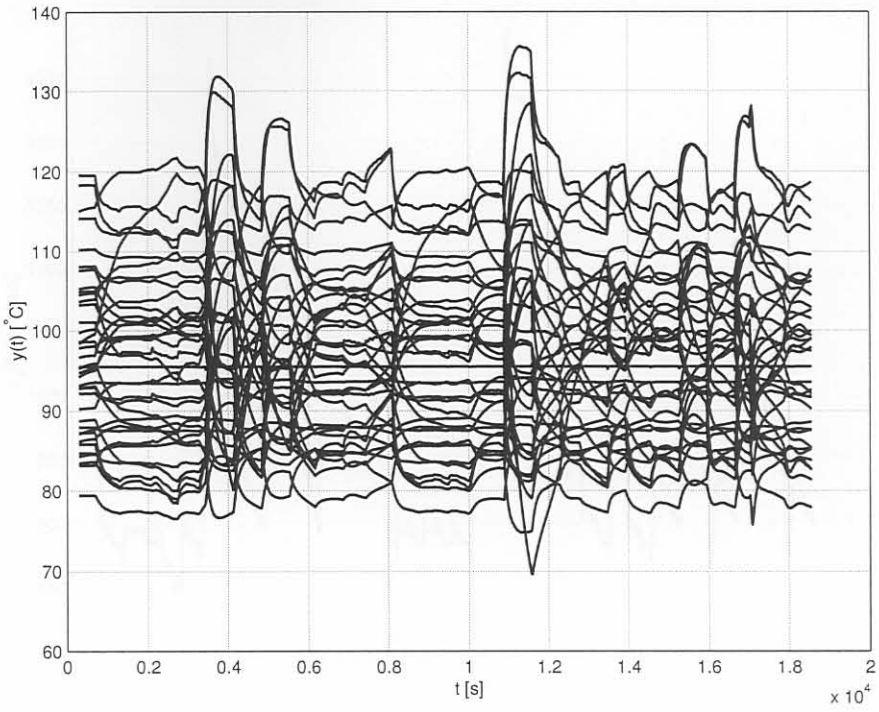

Figure 4.28 Thermocouple temperature outputs for 1060mm wide slabs when thermocouple in6u is used in a feedback configuration.

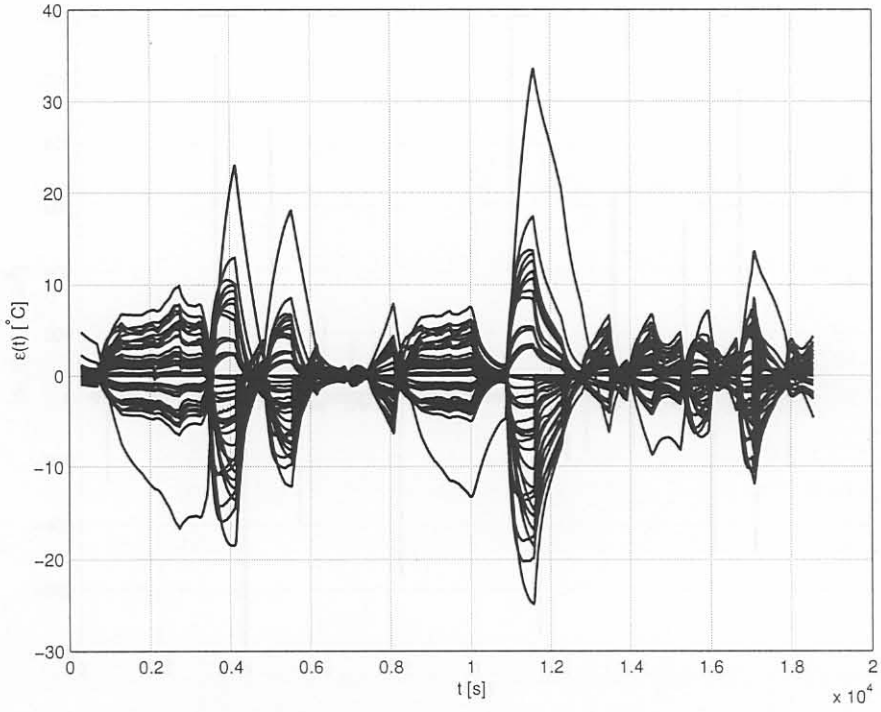

Figure 4.29 Thermocouple temperature errors for 1060mm wide slabs when thermocouple in6u is used in a feedback configuration.

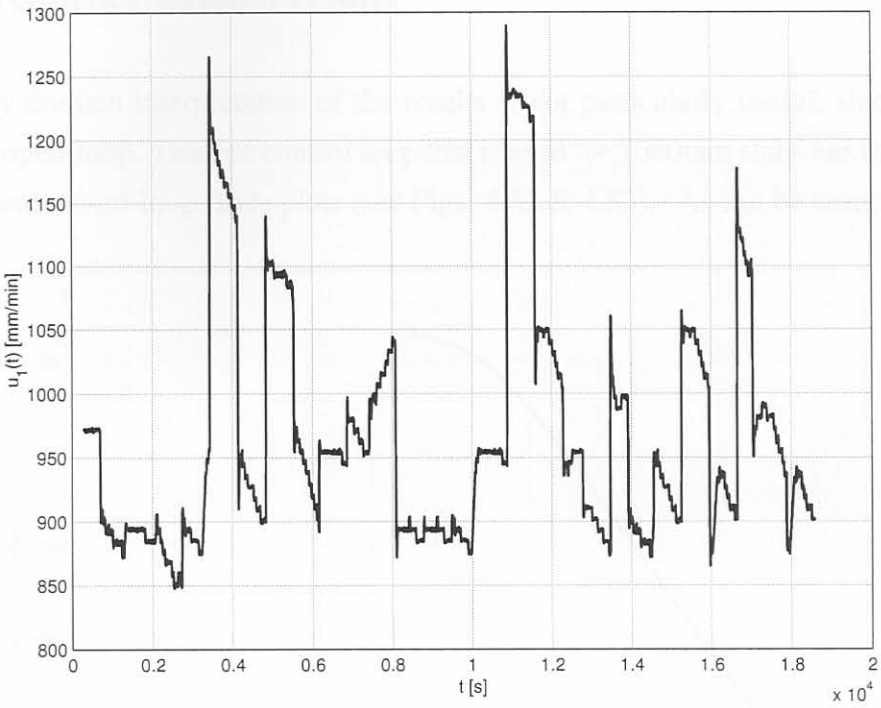

Figure 4.30 Control signal for 1060mm wide slabs when thermocouple in6u is used in a feedback configuration.

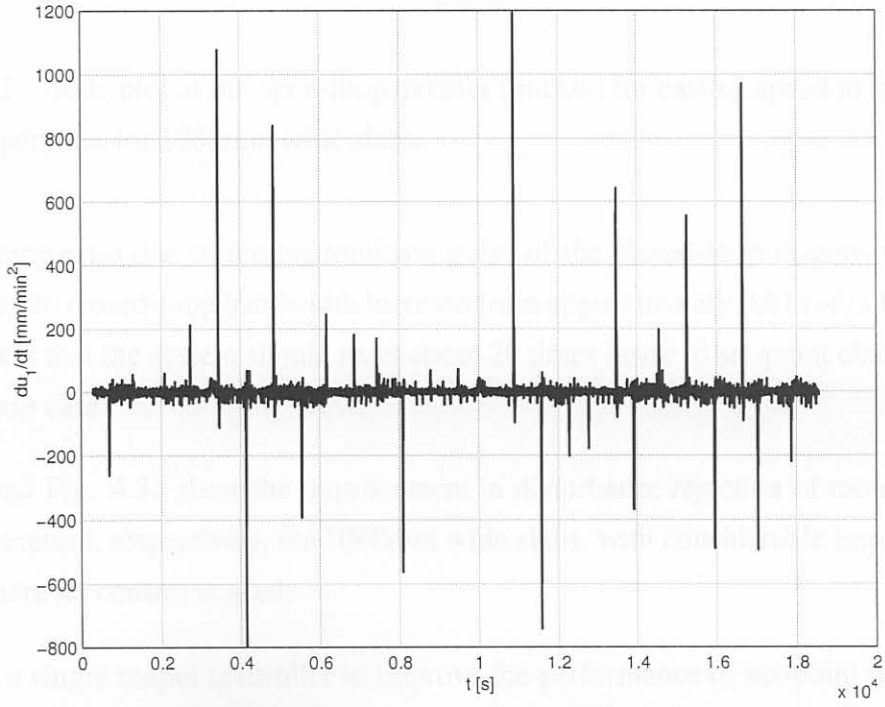

Figure 4.31 Slab acceleration for 1060mm wide slabs when thermocouple in6u is used in a feedback configuration.

4.2.3 Frequency-domain results

A frequency domain interpretation of the results is not particularly useful, since 37 of the outputs are open-loop. The one control loop that is used for 1060mm slabs has the following open-loop and closed-loop Bode plots (see Figs. 4.32 & 4.33). As can be seen, the approx-

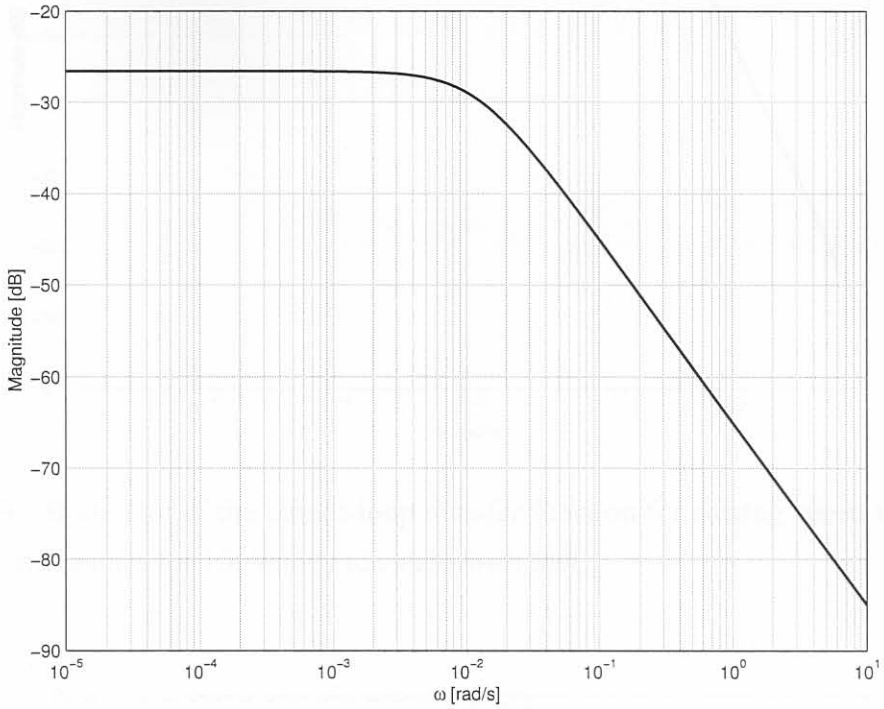

Figure 4.32 Bode plot of the open-loop transfer function for casting speed to in6u thermocouple temperature for 1060mm wide slabs.

imate damping ratio due to the predominant poles of the closed-loop response is 0.7 with an open-loop to closed-loop bandwidth increase from approximately 0.01 rad/s to 0.2 rad/s. This indicates that the system should react about 20 times faster to set-point changes than in the open-loop case.

Fig. 4.34 and Fig. 4.35 show the improvement in disturbance rejection of mould level and water temperature, respectively, for 1060mm wide slabs, with considerable improvement to the case where no control is used.

The use of a single output controller to improve the performance of set-point following for output disturbances was described. For 1060mm slabs, the improvement is approximately 23% over the case where no control is used. For 1280 and 1575mm slabs, the improvements are 39% and -2% respectively. The control has deteriorated when SOC is used on the 1575mm wide slabs and 1280mm wide slabs, compared with the LQTSS case. More results

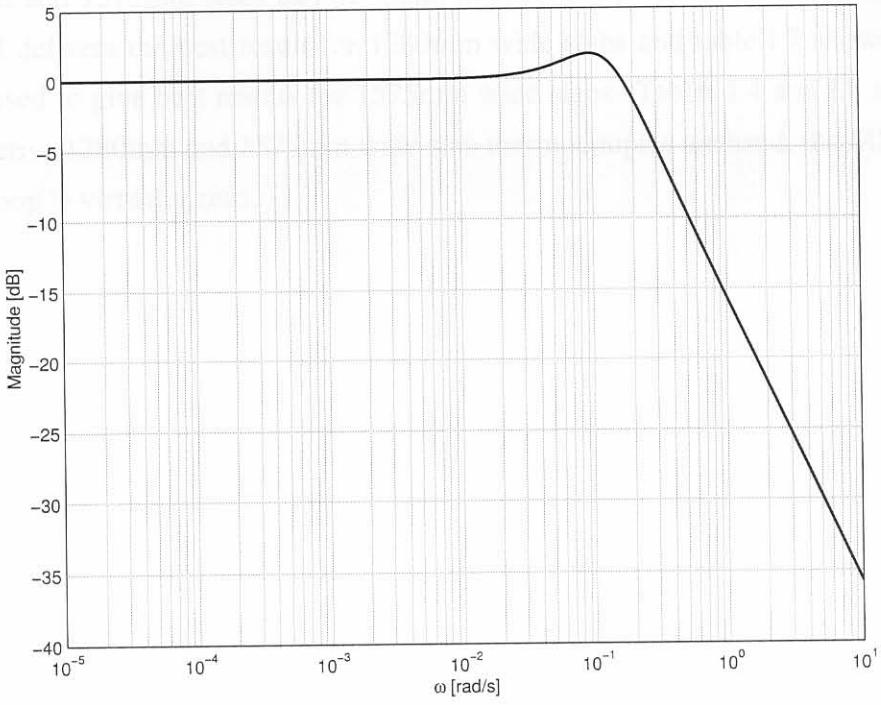

Figure 4.33 Bode plot of the closed-loop transfer function for casting speed to in6u thermocouple temperature for 1060mm wide slabs with SOC.

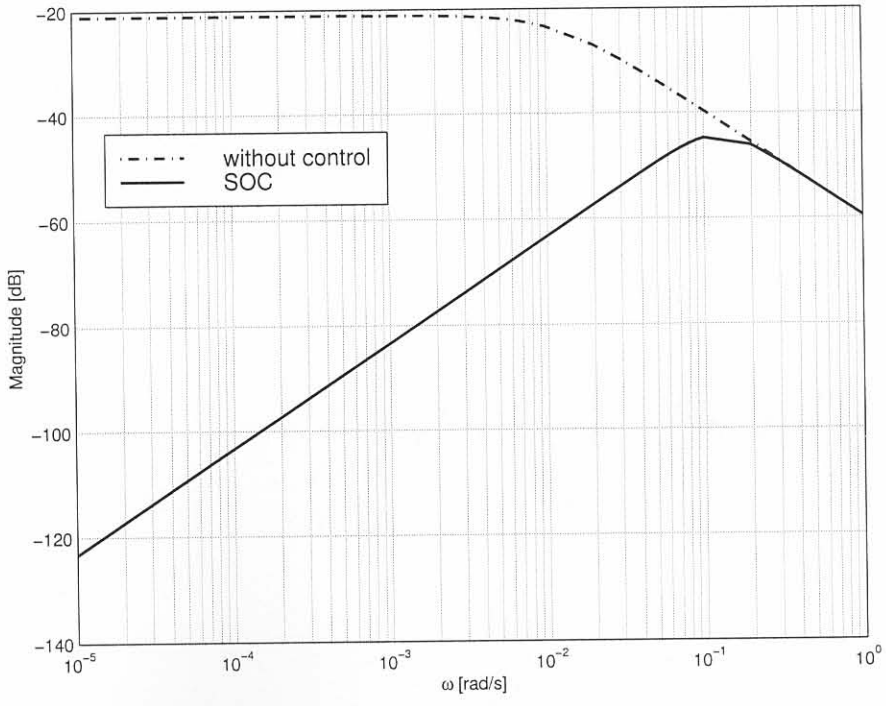

Figure 4.34 Bode plot of the rejection of the mould level disturbance for casting speed to in6u thermocouple temperature for 1060mm wide slabs using SOC.

for 1280mm and 1575mm slabs can be found in appendix I. Table I.3 shows that thermocouple ou2l delivers the best result for 1280mm wide slabs and table I.7 shows that ou5u should be used to give best results for 1575mm wide slabs. Tables I.4 and I.8 show that if these respective 1280mm and 1575mm wide slab thermocouples are used, the MSEs for that particular loop is virtually zero.

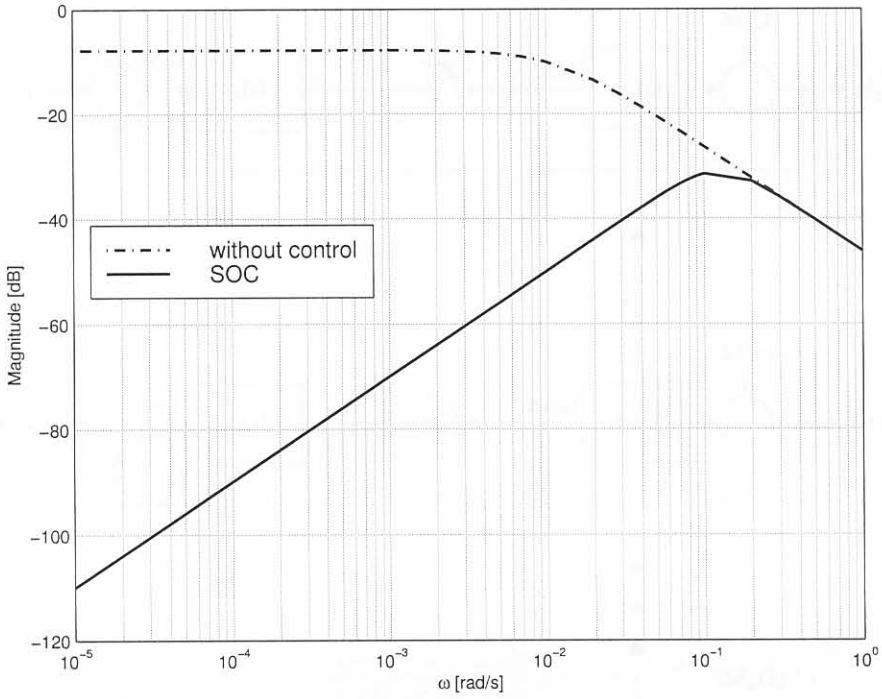

Figure 4.35 Bode plot of the rejection of water temperature disturbance for casting speed to in6u thermocouple temperature for 1060mm wide slabs using SOC.

4.3 Worst-case control (WCC)

This section describes the use of a worst-case control configuration. The basic idea is to utilize the SOC controllers, but to switch to the loop with the largest error. Fig. 4.36 shows the basic control configuration.

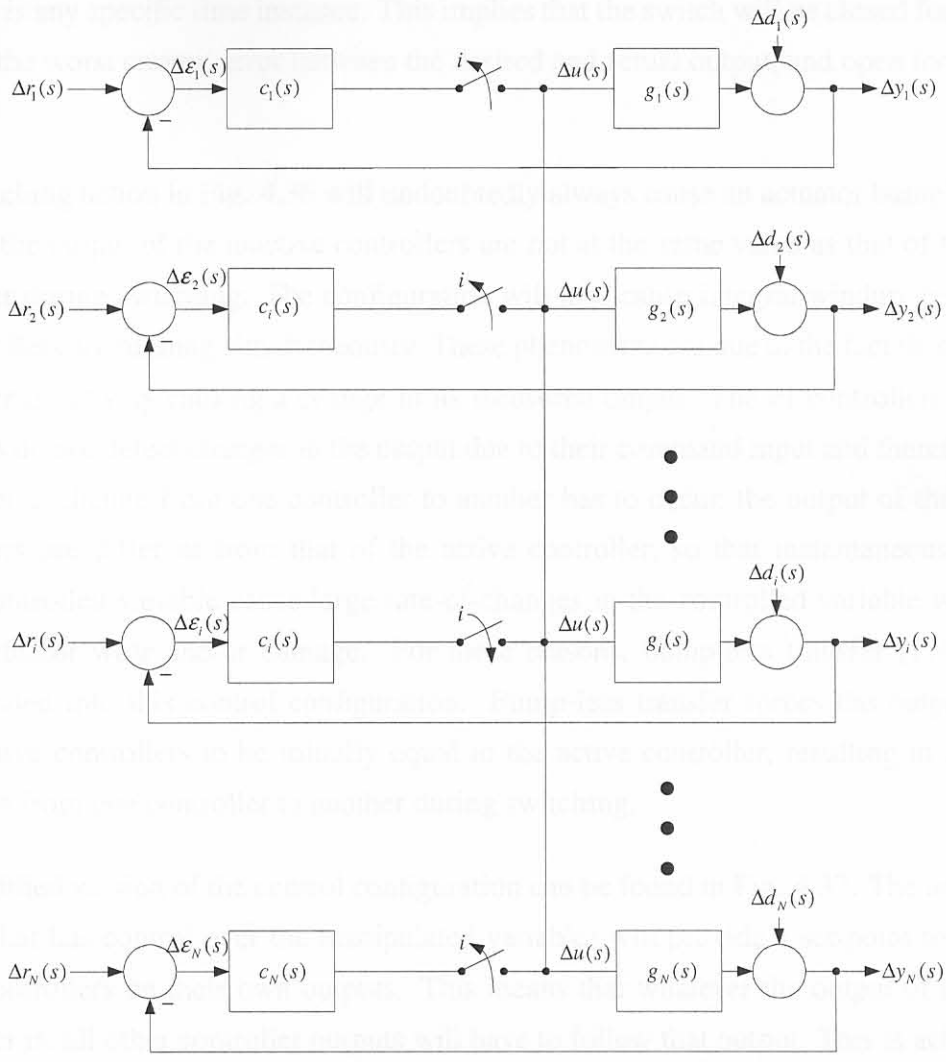

Figure 4.36 Control configuration for the worst case control method.

All variables and specifications are the same as in the SOC (§4.2).

4.3.1 Design overview

The switches between the controller output and manipulated variables are activated whenever the i-th output is performing the worst. During switching, the selected controller becomes

active and the remaining 37 controllers become inactive. This means that the casting speed is adjusted by the i-th controller whose loop output is the worst[m]. Mathematically, this can be written as follows and is known here as the switching criterion:

$$i = j|\max|\epsilon_j(t = t_1)|, \tag{4.10}$$

where t_1 is any specific time instance. This implies that the switch will be closed for the loop that has the worst current error between the desired and actual output, and open for all other loops.

The switching action in Fig. 4.36 will undoubtedly always cause an actuator bump to occur, because the output of the inactive controllers are not at the same value as that of the active controller during switching. The configuration will also cause integral windup, because all PI controllers are running simultaneously. These phenomena are due to the fact that only one controller is actively causing a change in its measured output. The PI controllers on 37 of the loops do not detect changes in the output due to their command input and therefore wind up. When a change from one controller to another has to occur, the output of the inactive controllers are different from that of the active controller, so that instantaneous changes in the controlled variable cause large rate-of-changes in the controlled variable which can cause actuator wear and/or damage. For these reasons, bump-less transfer [174] is also incorporated into this control configuration. Bump-less transfer forces the outputs of all the inactive controllers to be initially equal to the active controller, resulting in a smooth transition from one controller to another during switching.

The modified version of the control configuration can be found in Fig. 4.37. The active controller (that has control over the manipulated variable) will provide a set-point to all other active controllers on their own outputs. This means that whatever the output of the active controller is, all other controller outputs will have to follow that output. This is achieved by forming a feedback loop in parallel with the normal feedback loop of the controller $c_j(s)$. This new error signal $\gamma_j(s)$ is an input for the normal systems described in Fig. 4.36. Simultaneously, the WCC output feedback and set-points are disturbances for the bump-less transfer element (the controllers $c_j(s)$ look like plants to the bump-less transfer elements). Integral wind-up will also be eliminated because the purpose of the inactive systems is to follow the error between their output and the output of the active controller. Note that the active controller will not be adversely affected through the bump-less transfer because the bump-less transfer summation node subtracts the same signal from itself, thus providing an input disturbance of zero to the active controller.

[m] *i.e.* it has the largest absolute error between set-point and output

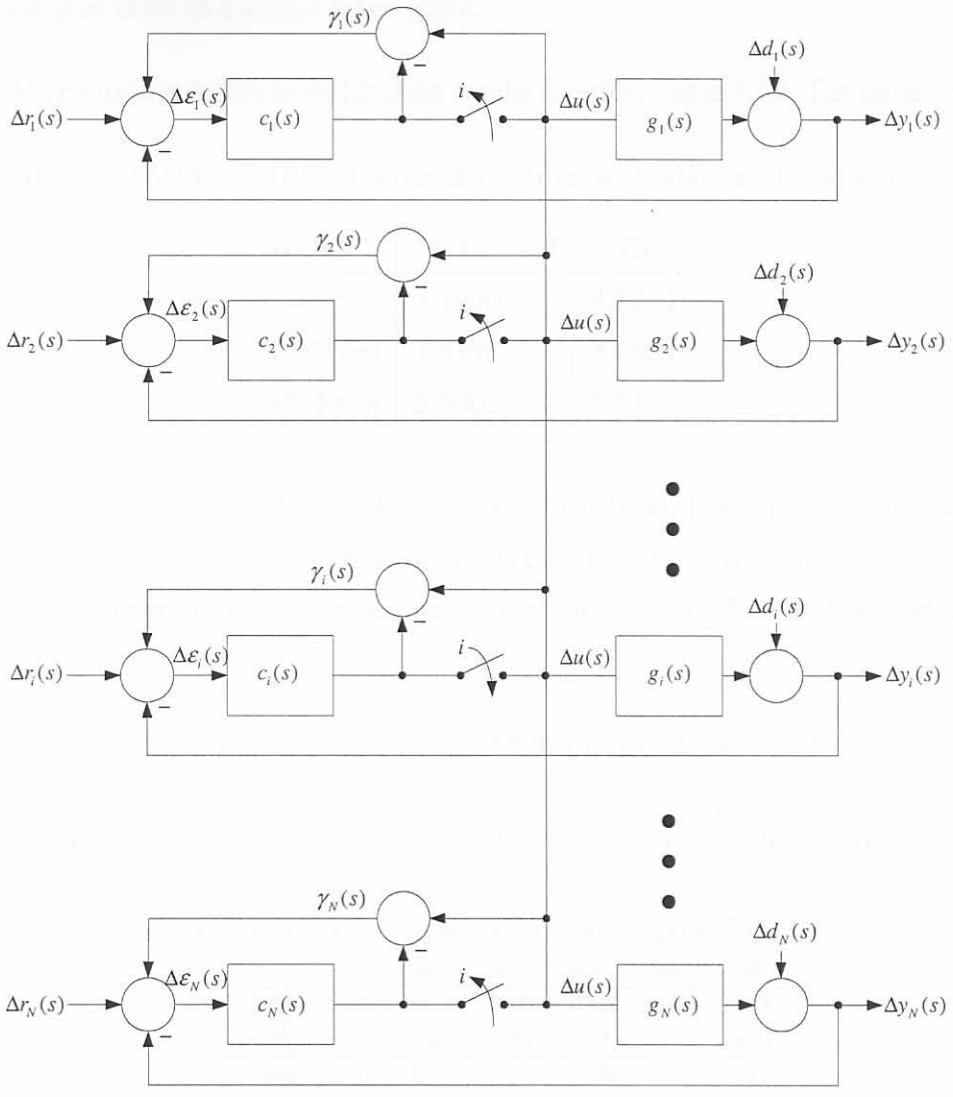

Figure 4.37 Control configuration for the worst case control method with bump-less transfer.

No extra dynamics have been added to the bump-less transfer system in order to keep the design simple. The loops increase in speed due to the $c_j(s)$ controllers. Because of the large response times of the system together with the actuator constraint, the inactive loops will adequately follow the active loop. Some dynamics can be added (see [174]).

Switches should not be placed in the WCC feedback path, because this will result in an actuator bump as soon as a switch takes place.

The SMSMSEs for the different width slabs can be found in Table 4.10. The table shows that

Table 4.10 SMSMSE for 1060, 1280 and 1575mm wide slabs with and without WCC.

Width	No Control	WCC
1060mm	5.1990	4.5012
1280mm	7.5198	5.1681
1575mm	5.5005	5.8138

there are improvements of 13.4%, 31.3% and -5.7% for 1060, 1280 and 1575mm wide slabs compared to no control respectively, using the WCC. The negative value for 1575mm wide slabs indicates a deterioration in the performance of the system. More will be said about this later (§4.4).

Table 4.11 shows the MSEs for each output when the worst-case control is used. These

Table 4.11 1060mm wide slab MSE for each output using the WCC.

in1u	in1l	in2u	in2l	in3u	in3l	in4u	in4l
21.37	5.488	27.12	35.86	12.79	20.39	8.627	2.928
in5u	in5l	in6u	in6l	in7u	in7l	in8u	in8l
8.364	3.087	5.428	11.63	8.376	4.823	15.1	4.78
ou1u	ou1l	ou2u	ou2l	ou3u	ou3l	ou4u	ou4l
68.57	4.345	27.56	10.9	81.65	66.52	23.79	30.94
ou5u	ou5l	ou6u	ou6l	ou7u	ou7l	ou8u	ou8l
1.796	5.351	NA	NA	7.603	85.99	49.74	8.629
nl1u	nl1l	nl2u	nl2l	nr1u	nr1l	nr2u	nr2l
1.496	3.067	5.818	52.93	2.659	4.88	23.63	5.882

figures show that the MSE ranges from very good values (*e.g.* 1.796 for ou5u) to very bad values (*e.g.* 68.57 for ou1u). This can probably be attributed to the fact that some outputs are above their reference values and some are below. This causes the control to decrease or increase depending on which loop is active, one above or one below the reference, with a net-effect of doing nothing to improve the overall response of the system.

4.3.2 Time-domain results

The following figures pertain to the 1060mm wide slabs. Results of 1280mm and 1575mm wide slabs can be found in appendix J.

Fig. 4.38 shows the mould level disturbance, $d_1(t)$, and Fig. 4.39 shows the water temperature disturbance, $d_2(t)$, used for simulation purposes. Fig. 4.40 shows the outputs when

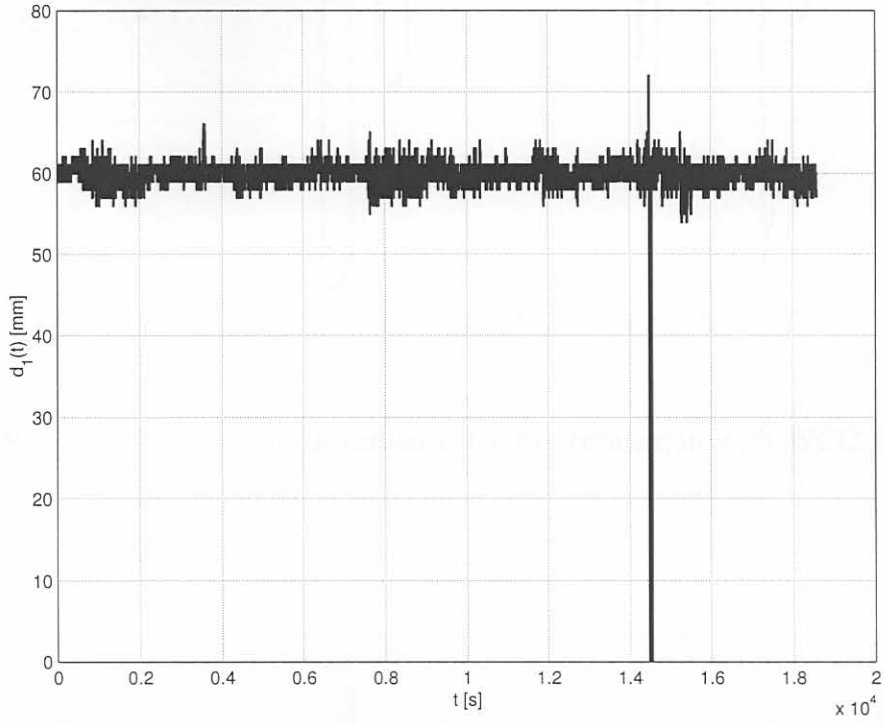

Figure 4.38 Mould level disturbance for the simulation with WCC for 1060mm wide slabs.

the worst-case control is used and Fig. 4.41 shows the tracking error on the output. These figures show a similar response to the LQTSS case for the specific disturbances, but peak values for temperature deviations are higher than in the LQTSS case.

Fig. 4.42 shows the control signal and Fig. 4.43 shows the acceleration of the slab. Fig. 4.44 shows the output of the switching criterion (*i.e.* which loop is active). These figures show that the casting speed remains below 1500mm/min, with the acceleration constraint being violated only twice, at approximately $t = 7000$s. Switching occurs mainly between loops 25 and 32 (*i.e.* thermocouples 25 and 32, see table 3.7 for a description of the indexes, i, for the thermocouples). These loops switch between each other because as one becomes active and tries to drive its negative output error to zero by increasing casting speed, the other loop's temperature also increases. The new controller then decreases the casting speed to drive

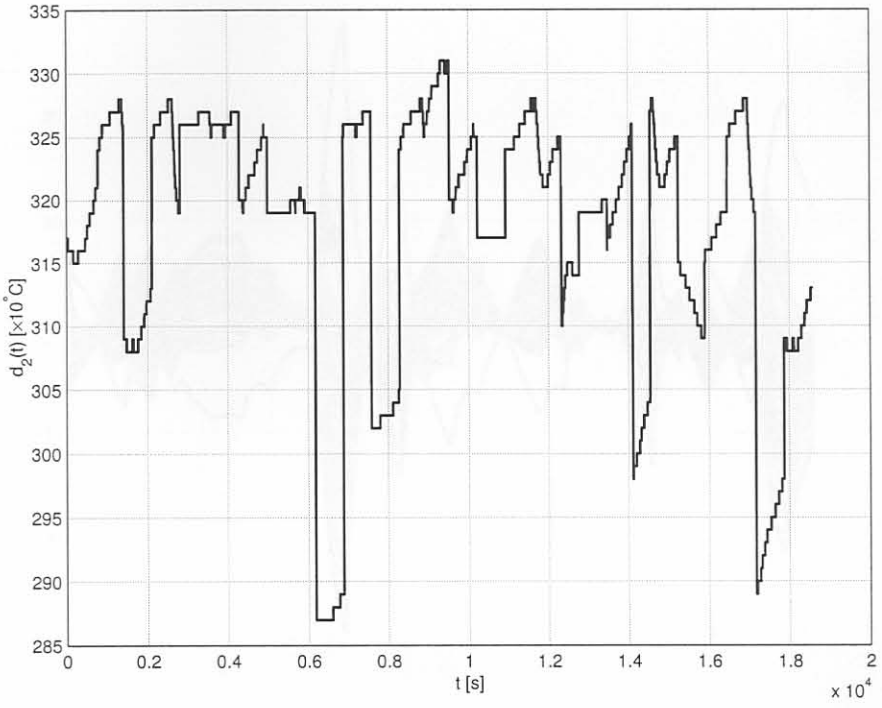

Figure 4.39 Water temperature disturbance for the simulation with WCC for 1060mm wide slabs.

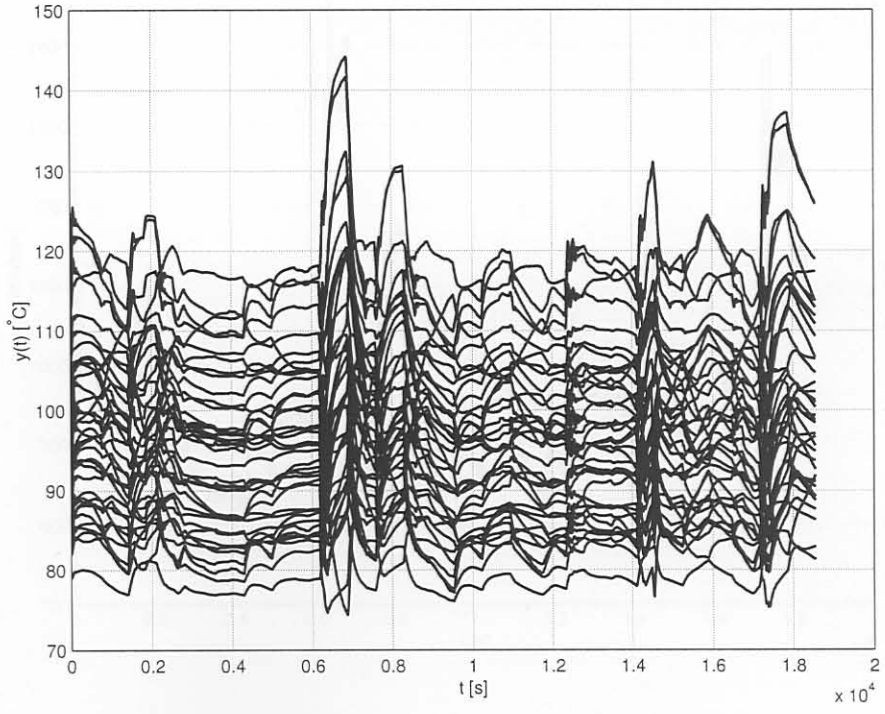

Figure 4.40 Outputs for 1060mm wide slabs and the worst-case control configuration.

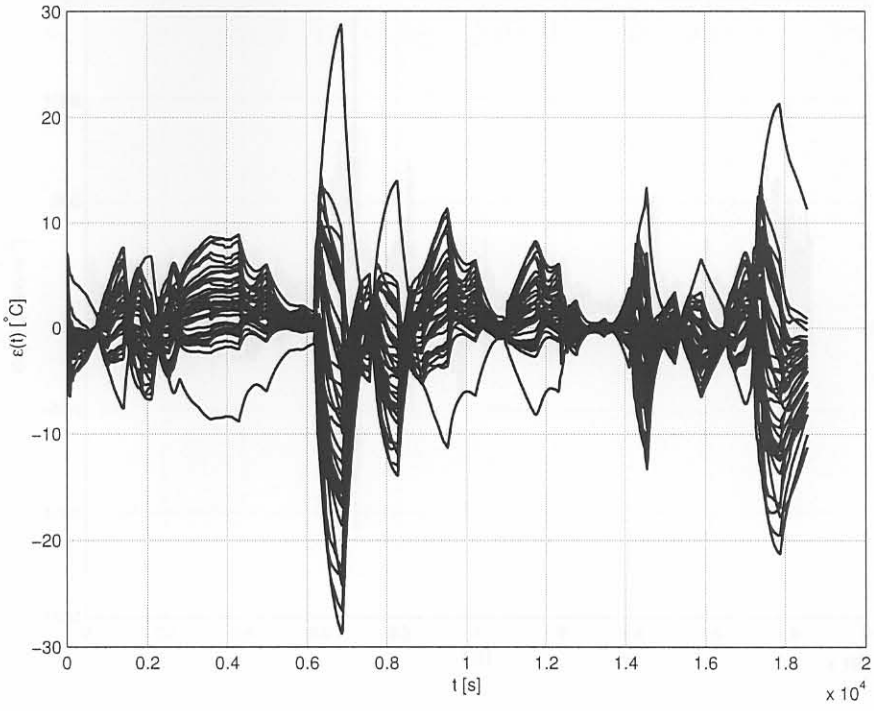

Figure 4.41 Errors for 1060mm wide slabs and the worst-case control configuration.

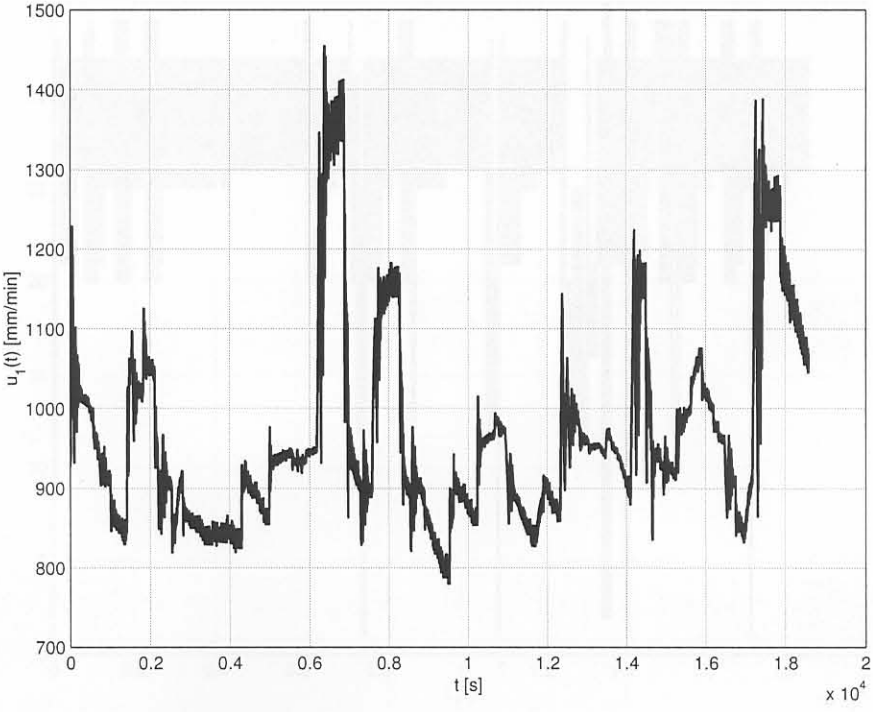

Figure 4.42 Control signal for 1060mm wide slabs and the worst-case control configuration.

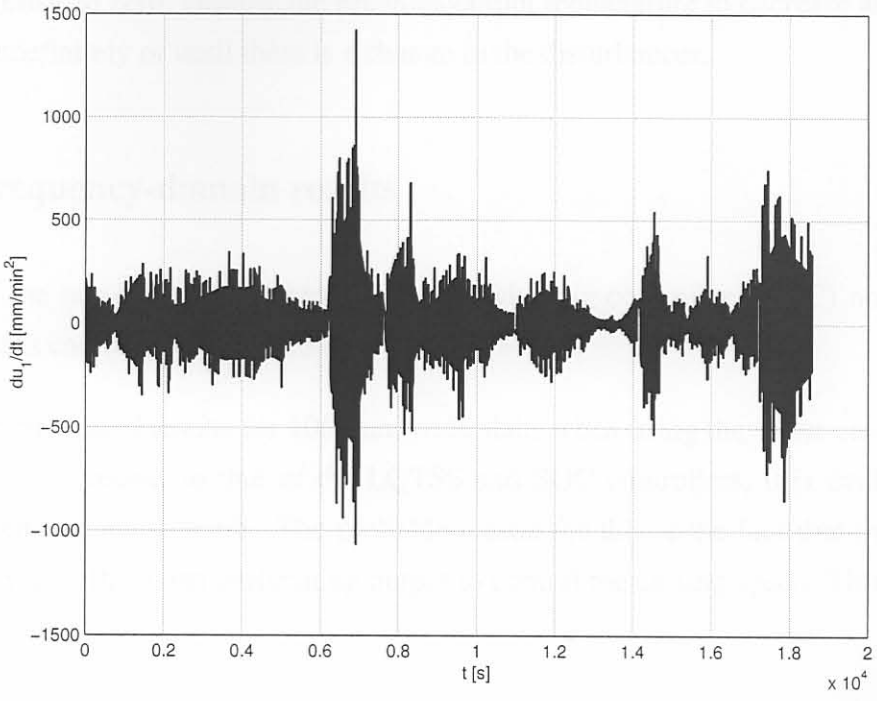

Figure 4.43 Acceleration of the slab 1060mm wide slabs and the worst-case control configuration.

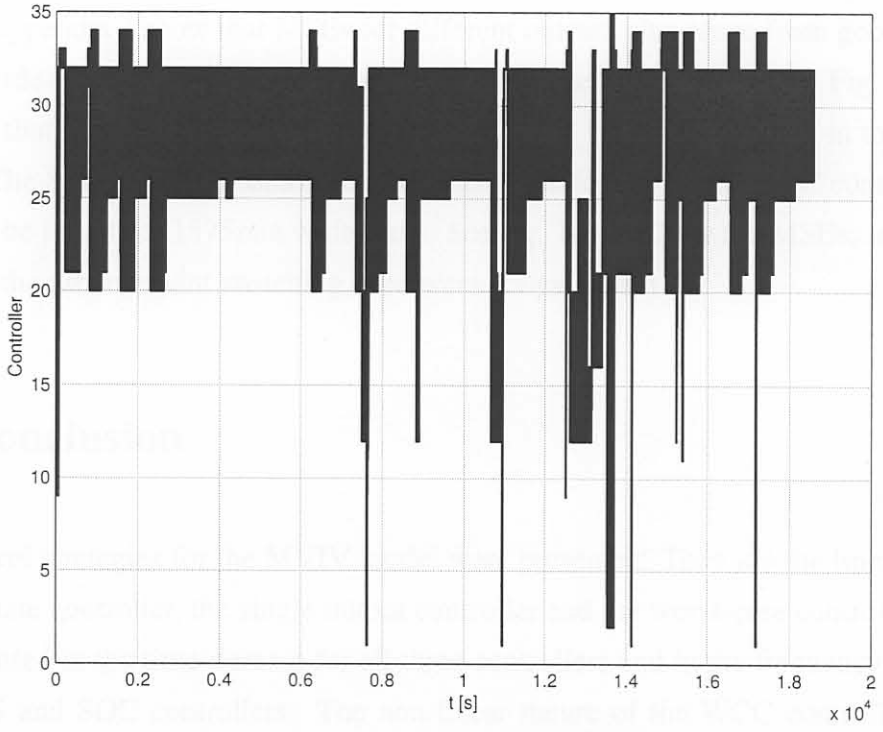

Figure 4.44 Output of the switching criterion of 1060mm wide slabs and the worst-case control configuration.

its positive error to zero, causing the previous output temperature to decrease and the cycle continues indefinitely or until there is a change in the disturbances.

4.3.3 Frequency-domain results

Because of the non-linear characteristic of the switching controller (WCC) no frequency-domain results can be given.

This section presented results for 1060mm wide slabs when using the worst-case controller. Comparing these results to that of the LQTSS and SOC controllers, it is evident that the WCC delivers the worst result. The probable reason for this is the fact that the controller continuously uses the worst performing output to control the casting speed. This means two things:

1. The active loop does not necessarily ensure the best control for all other loops.
2. The active loop is incapable to correct its output fast enough before it becomes inactive and switches to another loop.

Results in appendix J show that MSEs for different outputs also range from good to bad for 1280mm wide slabs (*e.g.* the in5u and nl2l loops in Table J.1 on page 287). Fig. J.6 on page 290 shows that alternation between control loops 8 and 19 is predominant in the switching criterion. The SMSMSE is in this case also worse than for LQTSS or SOC control. Similar results can be found for 1575mm wide slabs. See *e.g.* Table J.2 for the MSEs; and Fig. J.11 shows that the predominant switching is between loops 19 and 28.

4.4 Conclusion

Three control strategies for the MVIV model were presented. They are the linear quadratic at steady-state controller, the single output controller and the worst-case controller. Results were presented in the time-domain for all three controllers and in the frequency domain for the LQTSS and SOC controllers. The non-linear nature of the WCC controller does not permit a frequency-domain analysis of the controller.

Results in terms of the SMSMSE for each of the controllers with specific slab widths is presented in table 4.12. The table shows that the overall best controller is the LQTSS, with

improvements of 29.5%, 40.0% and 0.7% over the uncontrolled case for 1060, 1280 and 1575mm wide slabs respectively. The closest rival is the SOC controller with improvements of 22.5%, 38.9% and -2.2% for 1060, 1280 and 1575mm wide slabs respectively. This means that the LQTSS controller is 7%, 1.1% and 2.9% better than the SOC controller for the respective widths. The worst controller is the WCC with improvements of 13.4%, 31.3% and -5.7% for the respective widths.

The following conclusions can be drawn from table 4.12.

- Disturbances have a larger effect on the 1280mm wide slabs than 1060mm and 1575mm slabs. The SMSMSE for 1280mm wide slabs is much larger than that of 1060mm and 1575mm wide slabs in the uncontrolled case. This means that the operating conditions for 1280mm are further from the ideal than for the other two widths. The controllers can compensate for this incorrect operating condition of 1280mm wide slabs more effectively and thus the improvement is more dramatic.
- Traditionally, wider slabs have more surface defect problems than narrower slabs. This is evident from the few defects that occur on 1060mm wide slabs compared to 1280mm and 1575mm wide slabs. This means that narrower slabs are less sensitive to temperature changes.
- Less data were available for narrower slabs than for wider slabs, implying that defects occurred less frequently.
- There happened to be less defects on 1575mm slabs than on 1280mm wide slabs. This means that compensation is more dramatic for 1280mm wide slabs than for 1575mm wide slabs.
- Mould temperatures for wider slabs are more insensitive to casting speed changes. This is especially the case for 1575mm slabs where deterioration of the tracking per-

Table 4.12 Comparison of SMSMSE and improvements for each width and control method.

Width [mm]	No Control	LQTSS		SOC		WCC	
	SMSMSE	SMSMSE	Imp.	SMSMSE	Imp.	SMSMSE	Imp.
1060	5.1990	3.6632	29.5%	4.027	22.5%	4.5012	13.4%
1280	7.5198	4.5139	40.0%	4.597	38.9%	5.1681	31.3%
1575	5.5005	5.4614	0.7%	5.622	-2.2%	5.8138	-5.7%

formance has occurred for SOC and WCC. Limitations on casting speed and casting acceleration prohibits compensation for disturbances for the 1575mm slabs.